BRNO UNIVERSITY OF TECHNOLOGY
VYSOKÉ UČENÍ TECHNICKÉ V BRNĚ

FACULTY OF MECHANICAL ENGINEERING
INSTITUTE OF PHYSICAL ENGINEERING

FAKULTA STROJNÍHO INŽENÝRSTVÍ
ÚSTAV FYZIKÁLNÍHO INŽENÝRSTVÍ

DEPOSITION OF GA AND GAN NANOSTRUCTURES ON SILICON AND GRAPHENE SUBSTRATES

DEPOZICE GA A GAN NANOSTRUKTUR NA KŘEMÍKOVÝ A GRAFENOVÝ SUBSTRÁT

MASTER'S THESIS
DIPLOMOVÁ PRÁCE

AUTHOR
AUTOR PRÁCE
Bc. PETR MAREŠ

SUPERVISOR
VEDOUCÍ PRÁCE
Ing. JINDŘICH MACH, Ph.D.

BRNO 2014

Vysoké učení technické v Brně, Fakulta strojního inženýrství

Ústav fyzikálního inženýrství
Akademický rok: 2013/2014

ZADÁNÍ DIPLOMOVÉ PRÁCE

student(ka): Bc. Petr Mareš

který/která studuje v **magisterském navazujícím studijním programu**

obor: **Fyzikální inženýrství a nanotechnologie (3901T043)**

Ředitel ústavu Vám v souladu se zákonem č.111/1998 o vysokých školách a se Studijním a zkušebním řádem VUT v Brně určuje následující téma diplomové práce:

Depozice Ga a GaN nanostruktur na křemíkový a grafenový substrát

v anglickém jazyce:

The deposition of Ga and GaN nanostructures on silicon and graphene substrate

Stručná charakteristika problematiky úkolu:

Úkolem diplomové práce bude provést rešeršní studii růstu GaN strukturovaných materiálů na substrátu křemíku a grafenu. Student provede sérii depozic GaN na křemíkové substráty za vyšších teplot substrátu užitím efuzní cely a zdroje iontů dusíku o nízké energii (E<100 eV). Dále budou provedeny depozice GaN nanostruktur na substráty SiO2 modifikované užitím metody FIB. Dále budou provedeny série depozic Ga a GaN ultratenkých vrstev za různých fyzikálních podmínek (tok částic, teplota substrátu, energie svazku, …) na grafénové substráty. Takto vyhotovené vrstvy budou analyzovány metodami in-situ XPS, LEED a ex-situ AFM, SEM.

Cíle diplomové práce:

1)Provedení rešeršní studie rozhraní GaN a grafen.
2)Provedení rešeršní studie růstu nanostrukturovaných materiálů GaN v podmínkách UHV.
3)Depozice GaN na substrát modifikovaný užitím FIB.
4)Provedení série depozic Ga a GaN ultratenkých vrstev na grafenový substrát za různých fyzikálních podmínek (tok částic, teplota substrátu, energie svazku, …).

Seznam odborné literatury:

[1] Agnus G., Maroutian T., Fleurence a., Bartenlian B., Hanbu

Vedoucí diplomové práce: Ing. Jindřich Mach, Ph.D.

Termín odevzdání diplomové práce je stanoven časovým plánem akademického roku 2013/2014.

V Brně, dne 23.10.2013

L.S.

prof. RNDr. Tomáš Šikola, CSc. Ředitel ústavu	prof. RNDr. Miroslav Doupovec, CSc., dr. h. c. Děkan fakulty

ABSTRACT

The presented thesis is focused on the study of properties of Ga and GaN nanostructures on graphene. In the theoretical part of the thesis a problematics of graphene and GaN fabrication is discussed with a focus on the relation of Ga and GaN to graphene. The experimental part of the thesis deals with the depositions of Ga on transferred CVD-graphene on SiO_2. The samples are analyzed by various methods (XPS, AFM, SEM, Raman spectroscopy, EDX). The properties of Ga on graphene are discussed with a focus on the surface enhanced Raman scattering effect. Furthermore a deposition of Ga on exfoliated graphene and on graphene on a copper foil is described. GaN is fabricated by nitridation of the Ga structures on graphene. This process is illustrated by the XPS measurements of a distinct Ga peak and graphene valence band during the process of nitridation.

KEYWORDS

graphene, gallium nitride, gallium, SERS, nitridation

ABSTRAKT

Tato diplomová práce se zabývá studiem vlastností Ga a GaN nanostruktur na grafenu. Teoretická část této práce popisuje základní vlastnosti grafenu a GaN a problematiku jejich výroby s důrazem na význam grafenových substrátů pro růst Ga a GaN struktur. Experimentální část této práce se zabývá depozicemi Ga na grafen, který je připravený metodou CVD a přenesen na SiO_2. Tyto vzorky jsou studovány pomocí různých metod (XPS, AFM, SEM, Ramanova spektroskopie, EDX). Vlastnosti Ga na povrchu grafenu jsou diskutovány, zejména z hlediska povrchově zesíleného ramanova jevu (SERS). Následně jsou provedeny depozice Ga na exfoliovaný grafen a na grafen na měděné folii. GaN je připraven pomocí nitridace galliových struktur na grafenu. Tento děj je podrobně studován analýzou XPS měření výrazného Ga píku a valenčního pásu grafenu v průběho tohoto děje.

KLÍČOVÁ SLOVA

grafen, nitrid gallia, gallium, SERS, nitridace

MAREŠ, Petr *Deposition of Ga and GaN nanostructures on silicon and graphene substrate*: master's thesis. Brno: Brno University of Technology, Faculty of Mechanical Engineering, Institute of Physical Engineering, 2014. 69 p. Supervised by Ing. Jindřich Mach, Ph.D.

DECLARATION

I declare that I have elaborated my master's thesis on the theme of "Deposition of Ga and GaN nanostructures on silicon and graphene substrate" independently, under the supervision of the master's thesis supervisor and with the use of technical literature and other sources of information which are all quoted in the thesis and detailed in the list of literature at the end of the thesis.

As the author of the master's thesis I furthermore declare that, concerning the creation of this master's thesis, I have not infringed any copyright. In particular, I have not unlawfully encroached on anyone's personal copyright and I am fully aware of the consequences in the case of breaking Regulation § 11 and the following of the Copyright Act No 121/2000 Vol., including the possible consequences of criminal law resulted from Regulation § 152 of Criminal Act No 140/1961 Vol.

Brno ....

(author's signature)

ACKNOWLEDGEMENT

I would like to express my gratitude to my supervisor Ing. Jindřich Mach, Ph.D. for his helpful and valuable advices. I would like to also thank to Mgr. Vlastimil Křápek, Ph.D., prof. RNDr. Tomáš Šikola, CSc., prof. RNDr. Jiří Spousta, Ph.D., and Ing. Josef Polčák, Ph.D. for a tremendous help with the manuscript. My sincere thanks go also to Mgr. Dušan Hemzal, Ph.D and to Mgr. Petr Klenovský, Ph.D. for an amazing help with Raman spectroscopy. Special thanks go to my fellow labmates at the Institute of Physical Engineering at Brno University of Technology: Jan Hulva, Martin Konečný, Miloš Hrabovský, Kirill Ermakov, Petr Dvořák and Lukáš Břínek for astonishing advices and collaboration. I would like to also thank to the AMISPEC project, especially to the ON Semiconductor company for the support. I must also acknowledge the great help of my family.

Contents

Introduction

I present a study of properties of gallium and gallium nitride on graphene fabricated by chemical vapor deposition. The role of Ga and GaN for graphene research is significant due to exceptional properties of Ga on graphene and due to the importance of GaN-graphene interface for semiconductor device fabrication.

The study of metal nanoparticles (NPs) on graphene is attracting a lot of interest. They are useful for exploring the fundamental properties of graphene e.g. the interaction of graphene with light. The presence of metal NPs can enhance the performance of graphene-based sensors or solar cells. Furthermore, the metal NPs on graphene exhibit strong plasmonic effects such as surface-enhanced Raman spectroscopy and they can also functionalize the graphene. So far gold nanoparticles were studied nearly exclusively in this research area. However, gallium has very similar properties in this respect.

The motivation for the study of gallium nitride has its industrial background. GaN is a widely used semiconductor material which is traditionally used in optoelectronics and high power electronics. However, it is difficult to find a suitable substrate for the GaN growth. Several theoretical studies show that the graphene structure can serve as an epitaxial substrate. The experimental results have recently shown high-quality GaN layers on graphene grown with ZnO supporting nanostructures. Furthermore it has been shown that graphene can serve as a transparent electrode for GaN-based LED diodes.

My study connects the research of these two materials together. This was possible by a unique method of GaN fabrication. The method is based on the evaporation of Ga on a substrate which creates Ga structures on the surface. The next step is nitridation of these structures by a nitrogen ion beam. The Ga structures are then transformed to GaN crystals. The GaN deposition is therefore closely related to the properties of Ga on the surface.

For this reason the major part of my work focuses on the study of the properties of gallium on graphene. The Ga NPs exhibit a number of interesting properties on graphene and I will discuss them in the following text. I have focused on the behavior of the growth of Ga nanoclusters and also on the importance of Ga nanoparticles for graphene characterization. For this reason I have also studied the quality of the CVD graphene substrates. I also discuss the properties of the transformation of Ga NPs into GaN NPs.

The text is divided into several chapters. The theoretical part of the text starts with chapter 1. This chapter is focused on the fundamental properties of Ga and GaN. The methods of GaN growth and the difficulties of the GaN growth are discussed here.

Chapter 2 is dedicated to graphene. The elementary structure and also the problematics of its preparation are presented here. Part of the text is also focused on the characterization of graphene quality.

Chapter 3 is focused on the relation of the Ga and GaN to graphene. In both cases the recent scientific achievements are discussed. The gallium-gold analogy is shown and also the problematics of GaN growth on graphene is discussed.

The experimental part of my thesis starts in chapter 4. This chapter deals with the preparation of the CVD graphene on a copper foil. This is followed by the transfer of graphene onto various substrates. The quality of obtained graphene is evaluated.

Chapter 5 is the major part of the experimental work. Here the adsorption properties of gallium on transferred graphene are discussed. Several substrates for Ga growth are compared. Also the SERS effect of Ga nanoparticles is discussed.

Chapter 6 deals with the preparation of GaN nanostructures by the nitridation of Ga NPs. The mechanism of the process is presented here. The photoluminescence measurement of GaN and XPS measurements of graphene valence band are also shown.

1 | Gallium and gallium nitride

1.1 Gallium in present surface physics

Gallium is a soft silvery metal with the melting point at 29.76 °C, which is slightly above the room temperature. Therefore it was used in history as a temperature reference point and in thermometers. In 1875 it was isolated by electrolysis for the very first time by the French chemist Paul Emile Lecoq de Boisbaudran.

Nowadays, gallium is traditionally used in the electronic industry to produce versatile widespread semiconductors – gallium arsenide (GaAs) and gallium nitride (GaN). GaN and GaAs devices represent the most of the gallium consumption. Gallium is not found in a free form in nature. The production is done by smelting of various ores. The most used Ga-rich ore is bauxite. Bauxite is used for aluminum production but it contains ca. 50 ppm of gallium [1]. Apart from bauxite the zinc-rich ore (sphalerite) is used in Ga production as well. Gallium metal is also being obtained from GaAs and GaN scrap.

China, Germany, Kazakhstan and Ukraine are leading producers of gallium. In 2012 the world primary gallium production was estimated to be 273 tons with the price of 556 USD per one kilogram (for 99.9999 %-pure gallium)[1]. C.a. two thirds of Ga production is used for integrated cicuits and one third is used in optoelectronics – laser diodes, LEDs, photodetectors and solar cells (data from US).

Gallium is thus a widespread material in everyday electronics and therefore a lot of effort is made among researchers to study it's properties.

The gallium research follows its industrial applicability. Most of the researchers study the gallium arsenide and gallium nitride surfaces. A colossal work had been done in this field but there is a lot of papers in the field of elemental gallium as well. Because the focused ion beam (FIB) systems are nowadays really popular there are lots of recently published papers regarding the effects of FIB gallium source on various samples [2].

Number of papers are focused on the formation and structure of gallium spheres (droplets) on various surfaces [3]. Similar work had been also done at the Institute of Physical Engineering [4][5]. Gallium droplets were used for self-assembling of gold nanoparticles as well [6]. Micrometer-scale metallic Ga droplets were first coated with a monolayer of ligand-stabilized gold nanoparticles and then assembled onto a patterned electrode. Similar fluid-based methods have a potential for fabricating microscopic electronic devices. Self-assembling of gallium droplets

was also studied in [7]. GaAs quantum dots on GaAs substrate were used for site-selective formation of gallium droplets.

1.2 Gallium nitride in surface physics

1.2.1 Physical and chemical properties and applications of GaN

Gallium nitride is a binary III – V direct band gap semiconductor. It is a very hard and stable material with a wurtzite crystal structure (see Figure 1.1). Wurtzite structure is a binary hexagonal crystal system which is characterized by two lattice parameters: a and c. Other compounds such as SiC, ZnO, AlN, or BN crystallize in wurtzite structure too. GaN and its related compounds can crystallize in the zincblende structure as well but the wurtzite structure is more common. Crystallographically, they are related but show significant differences in the electronic properties. GaN has a high heat capacity and thermal conductivity. The wide band gap (3.4 eV at RT) makes it viable for a variety of applications (for basic characteristics see Table 1.1). It is widely used in high – power and high – frequency electronics like cellular base stations, satellites or power amplifiers. Like other III – nitrides GaN has a low sensitivity to ionizing radiation and therefore it is suitable e.g. for spaceborne applications.

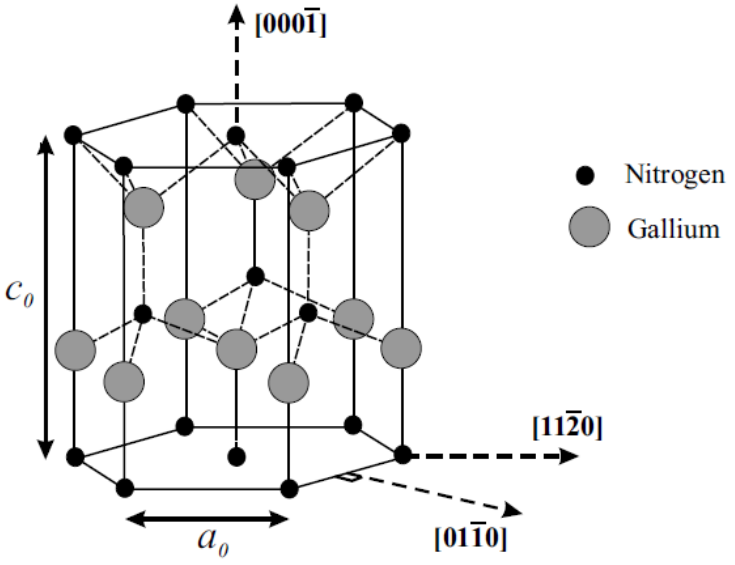

FIGURE 1.1: The wurtzite crystal structure of GaN [10].

Indium nitride (InN) with a band gap of 0.65 eV is used for indium gallium nitride (InGaN) alloys. These alloys (band gap can be theoretically tuned from 0.65 eV to 3.4 eV) cover the whole solar spectrum and they are perfect as a solar cell material. GaN's alloys with InN and AlN (bandgap 6.2 eV) were the leading contenders for solving the "green gap" problem – a range of wavelenghts (green to yellow) that have shown severely low-output efficiency by any other semiconductor emitter [9]. Devices based on these materials have competed in the past with

II-VI compounds such as ZnSe in light-emitting diode (LED) application. The GaN-based systems offered improved characteristics for both electronic and optical applications. See Figure 1.2 for further characteristics of Al-Ga-In nitrides. The main reason for their using in light emitting application is that their bandgap covers the entire visible spectrum. The other reason is the strong chemical bonding of the nitrides which makes the material very resistant to degradation (by high current or intense light illumination).

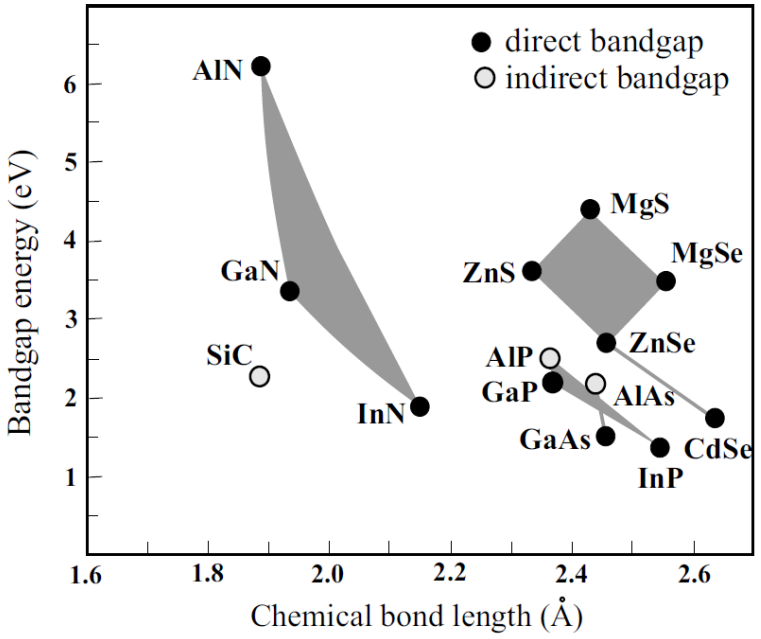

FIGURE 1.2: The bandgap energies and the chemical bond lengths of compound semiconductors that emit in the visible range of the electromagnetic spectrum [10].

In the early 1990s the research group of Shuji Nakamura developed a GaN-based blue light emitting diode. This was a breakthrough in a light-emitting industry because it was the key part for construction of white LEDs and in consequence it enabled manufacturing of full-color LED displays and blue laser devices [11]. GaN-based violet laser diodes are used to read Blu-ray Discs as well.

1.2.2 Substrates for the growth of gallium nitride

Gallium nitride is not an easy material to grow. Its high melting point temperature and high nitrogen pressure needed make severe inconveniences for the growth from the melt by Czochralski method [14]. At higher temperatures (starting at c.a. 800 °C) GaN can easily decompose which makes the growth difficult to achieve [15]. Bulk GaN crystals can only be grown from a solution of atomic nitrogen in liquid gallium at 1800 K at high nitrogen pressures (15 – 20 kbar [14]). These bulk crystals are extremely expensive and thus GaN is commonly grown by heteroepitaxial methods.

Bandgap energy (eV) [13]	E_g(300 K) = 3.39 E_g(1.6 K)= 3.47
Lattice constant (Å) [12] (T = 300 K)	a = 3.189 c = 5.186
Thermal expansion, linear (K^{-1}) [13]	Δ a/a = 5.59·10^{-6} Δ c/c = 3.17·10^{-6}
Number of atoms in 1 cm^3	N= 8.9·10^{22}
Density (g/cm^3) [13]	6.15
Thermal conductivity ($Wcm^{-1}K$) [13]	$\kappa = 1.3$
Melting point (°C) [13]	2500
Refractive index () [13]	2.3
Debye temperature (K) [13]	600

TABLE 1.1: Characteristics of GaN in a wurtzite structure.

A considerable effort was made to find a suitable substrate for a growth of a good-quality GaN. A number of materials have been studied for this purpose. The lattice mismatch between GaN and the substrate is the main criterion in a selection of a substrate. However, not only lattice constants are of a great significance, but also the structure of the crystal material, treatment of a surface composition, reactivity of the surface, as well as chemical, thermodynamic and electric properties of the material used, have a great influence on the heteroepitaxial growth [16].

Sapphire (Al_2O_3)

Sapphire(Al_2O_3) still remains the most used substrate for GaN epitaxy even though it has a large lattice mismatch (c.a. 16%). This results in high concetration of the mismatch dislocations (typically 10^{10} cm^{-2}). The thermal expansion coefficient of GaN is significantly lower that of sapphire. In consequence, this leads to cracking of the thick films. Sapphire is also an insulator which complicates a device fabrication because all electric contacts have to be mounted on the front side of the device [17]. The oxygen contained in sapphire can cause unintentional doping of GaN which could also be limitation for the fabrication of electric nanodevices [18].

Silicon carbide (SiC)

Another widely used substrate for the growth of GaN is silicon carbide (SiC). This material has several advantages over sapphire. At the first place SiC has the lattice mismatch of only 3.1 % [17]. It also has excellent thermal properties – its thermal conductivity is much higher then that of sapphire. It also provides a good electrical conductivity, which makes possible to mount the electrical contacts on the backside of the substrate. However the poor wetting between GaN and SiC makes the growth difficult. This can be overcomed by using a buffer layer. Usually a layer of AlN or $Al_xGa_{1-x}N$ compound is employed to improve the

layer properties. The lattice mismatch is low in comparison to sapphire but it still induces a considerable amount of dislocations.

Silicon (Si)

Considerable work was done on the growth of GaN on a silicon substrate. It is a very attractive material for GaN fabrication. Silicon wafers are very cheap due to a large scale production and the crystal quality of the Si wafers is excellent. Unfortunately the quality of GaN layers on silicon is usually worse than the quality of these layers on the previously mentioned substrates. Such a poor quality then decreases e.g. the luminescence efficiency. Nevertheless many GaN devices have been fabricated on silicon substrates even though there is usually a buffer layer needed [19].

Other substrates

Variety of other materials were used as substrates for GaN growth (e.g. GaAs or ZnO) with various results. In the following text I will discuss the possibilities of using graphene as a substrate or as a buffer layer for the growth of gallium nitride.

1.2.3 Growth of gallium nitride

Hydride vapor phase epitaxy (HVPE)

Several methods are being used for a preparation of gallium nitride on a desired substrate. The deposition of a single layer of GaN and AlN by means of hydride vapor phase epitaxy (HVPE) has been demonstrated more than 30 year ago. For GaN growth the source compounds are gallium chloride and ammonia gases. Gallium chloride is formed on the substrate inside the growth apparatus by a reaction of gaseous HCl and Ga metal [8] according to the equation

$$2\mathrm{Ga} + 2\mathrm{HCl} \rightarrow \mathrm{GaCl} + \mathrm{H}_2.$$

Layer of gallium chloride is in the next step transferred to another part of the growth system. The ammonia gas reacts here with gallium chloride which results in a layer of GaN on the surface. The deposition rate is of the order of several micrometers per minute. It makes the method useful for the growth of thick layers of GaN which can then serve as substrate for better quality epitaxial growth. Typical growth temperature varies from 900 to 1100 °C. During this process the III-nitride can be doped as a p-type or n-type semiconductor.

Metal organic chemical vapor deposition (MOCVD)

Rapid progress had been made in the early 1990s in the field of another epitaxial technology, metal organic chemical vapor deposition (MOCVD) or metal

organic vapor phase epitaxy (MOVPE). This method is now a leading technology for GaN fabrication.

It allows to produce a variety of materials but in case of GaN the method use a toxic gas trimethylgallium $Ga(CH_3)_3$ (TMGa) as a source of gallium. The method takes place at a moderate pressure (10 to 760 Torr) and the typical growth temperature is 1000 °C to 1200 °C [10]. The crystal is grown on a substrate by introducing TMGa and ammonia (NH_3). These precursors are brought into the furnace by carrier gases – hydrogen or nitrogen are usually used. The precursor gases decompose on the substrate and react according to equation:

$$Ga(CH_3)_3 + NH_3 \rightarrow GaN + 3CH_4.$$

This leads to a layer by layer formation of high-quality GaN on the substrate.

Molecular beam epitaxy (MBE)

Molecular beam epitaxy (MBE) requires a high vacuum or ultra-high vacuum equipment. Usually a base pressure better then 10^{-6} Pa is needed to achieve an impurity-free environment. MBE uses effusion cells as a source of gallium. The effusion cell (or an evaporator) is a device with a crucible inside. The crucible is filled with gallium (or other material which is supposed to be evaporated, e.g. Ti, Au, or Ag). The crucible is heated in UHV to the evaporation temperature where the material starts to evaporate. For Ga the temperature is around 800 °C . The heating is provided by a heated wire around the crucible or by a beam of electrons which are accelerated towards the crucible.

For the deposition of GaN a source of nitrogen has to be present as well. There are several options which are used as a nitrogen source. The nitrogen can be delivered to the surface by an ammonia molecule (similar to MOCVD). At higher temperatures (usually 800 °C) the NH_3 molecule decomposes and it can react with gallium atoms incoming from effusion cell [20]. This ammonia-based MBE was widely used in 1990s.

Other possibility is to use a radio frequency (RF) nitrogen plasma source which is a usual choice for the MBE-grown GaN. This source provides a wide low energy beam of highly reactive atomic nitrogen. Nitrogen is introduced into the discharge zone where the plasma is induced by the RF excitation. The nitrogen molecule is dissociated into nitrogen ions and neutral atoms. The ions stay in a discharge zone while the neutral atoms are effusing towards a sample and react with Ga atoms adsorbed on the sample.

At the Institute of Physical Engineering an electron-impact nitrogen ion source is used for GaN crystals fabrication [59]. The main chamber of the source is filled with a high-purity nitrogen gas. Part of the molecules is ionized by an accelerated electrons and the molecular ions are afterwards extracted from the source towards the sample with a low accelerating voltage (around 50 eV). The molecule of nitrogen then dissociates on the surface of the sample and it reacts with Ga atom forming GaN.

1.2.4 GaN nanostructures

Following chapter will mostly deal with the problematics of GaN nanowires. The field is intensively studied and GaN nanowires represent the biggest group of GaN functional nanostructures. Part of the work on this diploma thesis was connected to this topic as well. However, these experiments were not promising so I have moved from GaN nanostructures to the research of Ga and GaN properties on graphene. Nevertheless I will briefly mention the GaN nanowires work as well. The methods used and the experimental settings are explained later in the text.

Semiconductor nanowires are in general promising structures and they are expected to have a wide range of applications in photonics, electronics or even in the life sciences. The bottom-up fabricating of nanowires using a metal catalyst is nowadays the most frequent technology [21]. This method is described by VLS mechanism first described by Wagner and Ellis with silicon whiskers grown with a gold catalyst [22]. A liquid metal particle acts as a preferential sink to collect material from the semiconductor gas precursor.

In case of gallium nitride the metal catalyst is most frequently gold [23]. However, this approach has several difficulties. The foreign metal catalyst (e.g. gold) can incorporate into the wire which introduces internal defects and has a direct effect on the electronic device performance. A gallium metal itself can be used as a catalyst which prevents a contamination of GaN [24]. This self-catalytic approach is getting a high interest nowadays.

GaN nanowires can be grown without a metal catalyst as well. I was especially interested in the nanowhisker growth by molecular beam epitaxy without a metal catalyst. In 2009 Fernández-Garrido has introduced the growth diagram of nanocolumns fabricated by plasma-assisted molecular beam epitaxy [25]. The growth was performed on Si(111) samples. The diagram was established as a function of growth parameters exhibiting the transition between different regimes of growth (see Figure 1.3). It shows a temperature window where the nanowire growth occur. Outside of this window only the growth of a compact GaN layer or no growth can occur.

As presented in Ref. [25], the GaN nanowires grow in nitrogen-rich conditions (Ga/N flux ratio$<$1) at high temperature (c.a. 800 °C). In Fernández-Garrido's work the samples were grown at various temperatures (730 – 850 °C) and the impinging Ga deposition rate was varied (Φ_{Ga}=0.7 – 9.8 nm/min) while the active nitrogen deposition rate was kept stable (Φ_{N}=6nm/min). This work was the main motivation for our experiments. In Garrido's work the nitrogen RF source was used to produce GaN. To our knowledge there are no attempts of using an electron-impact ion source for GaN nanowires growth.

For this reason I repeated the growth procedure of Ref. [25] with a nitrogen electron-impact ion source. I have used bare Si(111) substrates. These substrates were annealed in ultra-high vacuum at 1300 °C to clean all the impurities. I have then used a conventional gallium effusion cell as a Ga source. I have used high Ga fluxes to maintain a sufficient supply of gallium on the sample (200 nA was measured in the evaporator). As a nitrogen source I have used an electron-impact source which was able to provide a beam of N_2^+ ions with a current density of 2 μA/cm^2 (measured by Farraday cup) and energy of 30 eV. At these

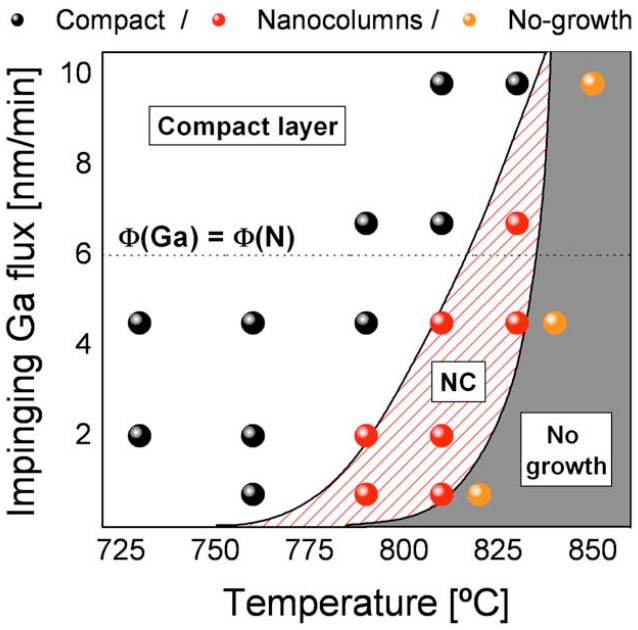

FIGURE 1.3: Nanowires growth diagram showing the boundary between compact and nanocolumnar regimes as a function of impinging Ga flux (deposition rate) and temperature for constant value of impinging nitrogen atoms. The growth of the nanowires was possible just in a small "window" between the region of compact layer of GaN and the region where no GaN growth occured [25].

conditions I have been depositing GaN for 60 minutes at various temperatures: 690 °C, 750 °C, 780 °C, 810 °C, 840 °C. I have chosen these temperatures to cover the "temperature window" from Fernandez-Garrido's work.

With this approach I have not obtained any nanowires. We have obtained at all our samples a layer of GaN without any signs of GaN nanocolumns. The samples were measured by X-ray photoelectron spectroscopy (XPS) and scanning electron microscope (SEM). There are several reasons for such a result. The main problem is that we have used an optical pyrometer to measure the temperature. The deviation of such measurement can be high if the emissivity of the substrate is not known precisely. The other possible reason is that I was not able to measure the impinging Ga flux properly. For a precise measurement of this value the QCM (quartz crystal microbalance) device must be used to calibrate the measurements but this was not available in our deposition setup. The use of the electron-impact ion source instead of a RF source can affect the results as well. In general the RF ion sources are producing much higher ion current. It is therefore possible that we could not sustain the suitable Ga/N ratio.

This study was suspended because after performing these experiments a vacuum leak was discovered in a central UHV chamber and this was being fixed for several weeks. Afterwards we have moved the research topic towards the study of gallium/graphene interface.

2 | Graphene

Graphene is a one atom thick two-dimensional layer of carbon atoms bound in a hexagonal lattice structure [27]. It has been extensively studied in the last several years since it was isolated for the first time in 2004 [26]. The high interest in graphene is caused primarily due to a number of exceptional properties it possesses.

Graphene can be described as a one-atom thick layer of graphite which is sufficiently isolated from its environment to be considered free-standing [28].

Graphene has an exceptional band structure thanks to its crystal structure. The distance between the closest carbon neighbors is about 1.42 Å and each carbon atom shares a σ bond with its three neighbors [27]. The fourth valence electron is responsible for a π bond which is oriented out of the plane.

2.1 Synthesis of graphene

For the very first time graphene was isolated using the famous Scotch tape method. Many processes have been developed for manufacturing a single or a few-layer graphene. The biggest issue for graphene fabrication is producing samples with a low density of defects and with a high charge carrier mobility. For such samples the mechanical exfoliation is the method of choice. However it is time consuming and limited to a small scale production. Table 2.1 shows summary of the most important synthesis methods.

2.1.1 Exfoliated graphene

This was the first method graphene was obtained with and it was developed by Geim and Novoselov [26]. The original idea was that one can get a well-defined 2D material just by mechanical splitting of a layered 3D material – graphite. For graphene fabrication a highly oriented pyrolytic graphite (HOPG) is used as a sample. In case of [26] the HOPG was etched by an oxygen plasma.

Method	**Layers**	**Size**	**Mobility** ($cm^2V^{-1}s^{-1}$)
Exfoliation	1 to 10+	1 mm	15000
Thermal SiC	1 to 4	50 μm	2000
Ni-CVD	1 to 4	1 cm	3700
Cu-CVD	1	65 cm	16000

Table 2.1: Comparison of the most popular graphene fabrication methods.

The etching created a small mesas on the HOPG and these mesas were pressed into a layer of photoresist. The photoresist was baked afterwards and the HOPG was removed from the resist. A Scotch tape was used repeatedly to peel the flakes of graphite from the mesas. The Scotch tape was then dissolved in acetone and the graphene flakes were captured on the surface of a silicon wafer with 300 nm of SiO_2. See figure 2.1 for the image of flake made by this method.

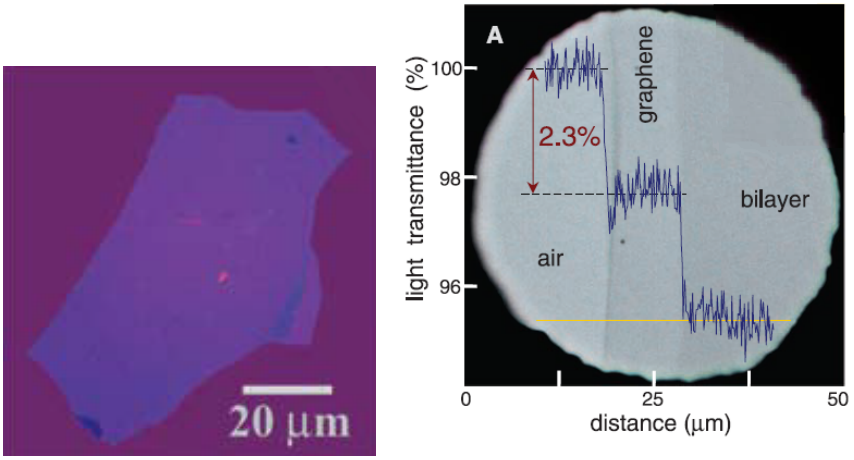

FIGURE 2.1: Left – Multilayer graphene flake with the thickness of c.a. 3 nm on top of a Si wafer with 300 nm of SiO_2 [26]. Right – Optical microscopy image of monolayer and bilayer graphene. The inset shows a measurement of the light transmittance of these materials.

The flakes are afterwards identified by an optical microscope using the contrast difference. The intensity of a transmitted light is decreased by 2.3 % [29] by one layer of graphene. One can identify by this method a few-layer graphene (FLG) as well. See Figure 2.1 for a detailed image. Graphene made by this method is of excellent quality. It is used mostly for studying the elementary properties of graphene. However the process is limited to very small sizes and it cannot be used for an industrial graphene production.

2.1.2 Thermal decomposition of SiC

A large scale single to few-layer graphene can be fabricated epitaxially on SiC by thermal decomposition. The SiC wafer is used and heated at high temperature (usually in ultra-high vacuum at temperatures 1000 °C – 1500 °C). Silicon atoms desorb from the surface while the carbon atoms stay on the surface and the whole sample surface is grafitized and a single to few-layer graphene is formed on the surface. The final surface structure of such system strongly depends on the annealing and cooling conditions of SiC samples and it is a great challenge to control these properties. Sometimes a high Ar pressure (c.a. 900 mbar) is introduced and this can reduce the surface roughness and enables a large-scale growth. For characterization of the thickness of graphene layers a low energy electron microscope (LEEM) can be used. In LEEM the graphene layers are providing a different contrast information due to the interference of the backscattered electrons – see Figure 2.2 [30].

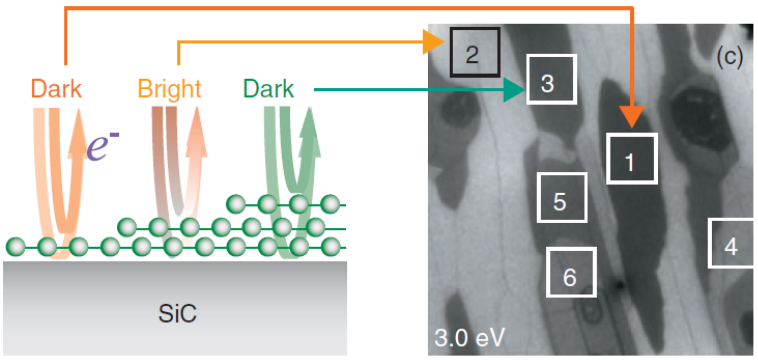

FIGURE 2.2: The graphene on SiC which is imaged by a low energy electron microscope (LEEM). Electrons reflected from the graphene surface can interfere which causes the electron reflectivity to change periodically as the function of energy and graphene thickness [30]. The numbers in the image show a number of graphene layers on the imaged area.

The thermal decomposition of SiC is exceptionally interesting because SiC itself is a wide band-gap semiconductor and it can suit well for electronics applications which can be fabricated using the SiC/graphene interface. However, such applications were still not realized. For the research of graphene properties it is really difficult to gain a large scale graphene sample which can be transfered onto a different substrate. The graphene transfer is a big issue and a reliable method for a large-scale graphene transfer has not been found yet.

2.1.3 Chemical vapor deposition

Carbon can be delivered to the substrate also from a gas form. The deposition takes place in a reactor where the hydrocarbon precursor gas is fed into at high temperature (around 1000 °C). The synthesis is performed with metal substrates and the most popular for graphene growth is nickel and copper. The hydrocarbon gas precursor is passing through a hot zone where it decomposes to carbon residues at the metal substrate surface and then forms a thin layer of graphene (single to few layer)[34]. The metal acts like a catalyst to lower the energy of the reaction and it also determines the deposition mechanism. This approach is the most promising for graphene production because it is inexpensive and a large-area graphene can be obtained. I will briefly discuss the CVD graphene growth on nickel and then I will proceed with a deposition on copper, because that was the method I have used for CVD graphene preparation.

2.1.3.1 CVD synthesis of graphene on nickel

At first the polycrystalline nickel substrate is annealed in Ar/H_2 atmosphere. The mechanism of graphene formation on nickel involves first methane decomposition on the catalytic surface. This happens usually in an Ar/H_2 atmosphere where the hydrocarbon precursor gas (most frequently methane) is injected. The depositions takes place at high temperatures (c.a. 700 – 1000 °C) [32]. In the second step the carbon is dissolved in nickel. The final step is precipitating of

carbon on the nickel surface during the cooling due to the decrease of carbon solubility in the nickel bulk. This ends with a graphitized layer on the surface. Another precursors like acetylene, ethylene or ethanol were used for the graphene fabrication on nickel. This method is able to produce one to a few-layer graphene [32].

2.1.3.2 CVD synthesis of graphene on a copper foil

CVD synthesis of graphene on a copper foil is the most common method for graphene fabrication and it is also used at the Institute of Physical Engineering. The synthesis process is quite similar to the growth on nickel. The reaction takes place in the same type of reactor. Copper has several advantages for graphene growth over nickel. At high temperatures the carbon atoms diffuse into the nickel bulk which is rather difficult to control. There is no such effect on copper surface. The graphene layer is formed directly on the surface during the hydrocarbon precursor dissociation and the carbon atoms do not diffuse into the copper bulk. Furthermore it was found that the graphene grown on copper substrates is primarily monolayer independent of the growth time. This indicates that the process is surface mediated and self limiting [27]. This makes the growth process significantly easier. This method is efficient for one layer graphene growth. The growth of large graphene sheets (in range of several centimeters) is possible with this method.

The substrate itself is important as well. Most frequently a thin 25 – 100 μm copper foil is used but an ultrathin copper layer made by ion sputtering is used for the research purposes as well. The basic mechanical properties are also important for latter growth. For example the polishing of the foil has a strong effect on the nucleation properties and the impurity particles introduced during the polishing can also play a crucial role [33]. In general it is important to have as flat and clean copper surface as possible for graphene synthesis.

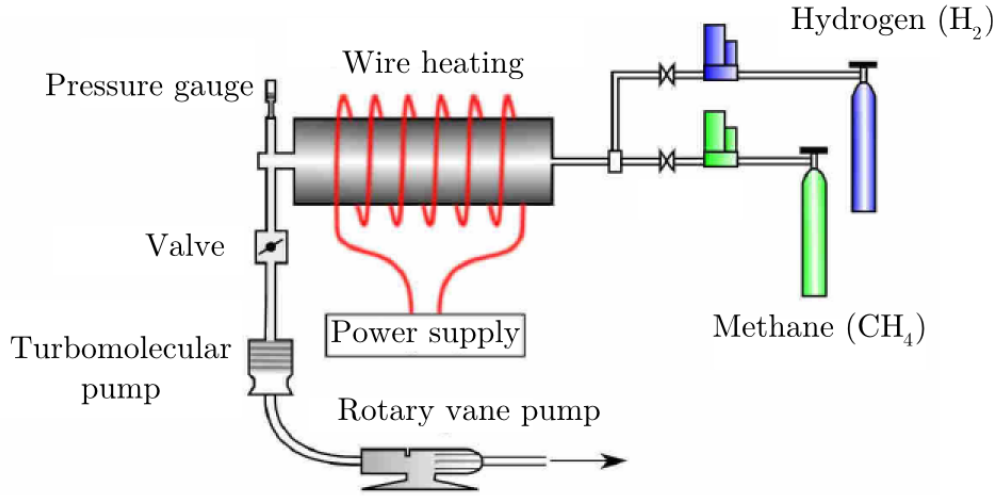

FIGURE 2.3: The growth chamber used at the Institute of Physical Engineering [34].

The growth is performed at the temperature around 1000 °C at low pressure ($10^0 - 10^1$ Pa) in several steps. The procedure takes place in a reactor with

several inlet valves (see Figure 2.3). At first the substrate is annealed in hydrogen atmosphere. Afterwards a precursor gas, usually methane, is introduced into the chamber. The gas reacts with the heated copper surface which catalyzes the reaction and a graphene is starting to form. Nucleation starts at suitable sites, e.g. minor defects in copper structure or even at the artificial scratches. Graphene then starts to form islands on the surface. In case of 2D material the more appropriate term for the island is a flake. Graphene flakes are getting bigger until they finally merge forming a layer of graphene all over the copper surface. The procedure can be stopped during this process and this results in obtaining a copper surface with graphene flakes. The third step is cooling of the sample. Growth on copper foil is resistant to the changes of a cooling speed, mainly due to the low carbon solubility in copper. This is another advantage over the growth on nickel where the cooling speed does have a crucial effect on the graphene synthesis.

2.1.4 Transfer of graphene onto a different sample

I will discuss the transfer of a CVD graphene in this section. The transfer of graphene after the deposition is an important step. It is needed for the characterization of its electronic properties or for the electronic device fabrication. For this purposes it needs to be transferred onto some desired insulating substrate (most frequently Si/SiO_2). So far the most popular idea of the CVD graphene transfer is to etch the copper foil away – this is the reason why the foil is so thin. After the etching one can obtain a free standing graphene membrane which can be placed on a desired substrate.

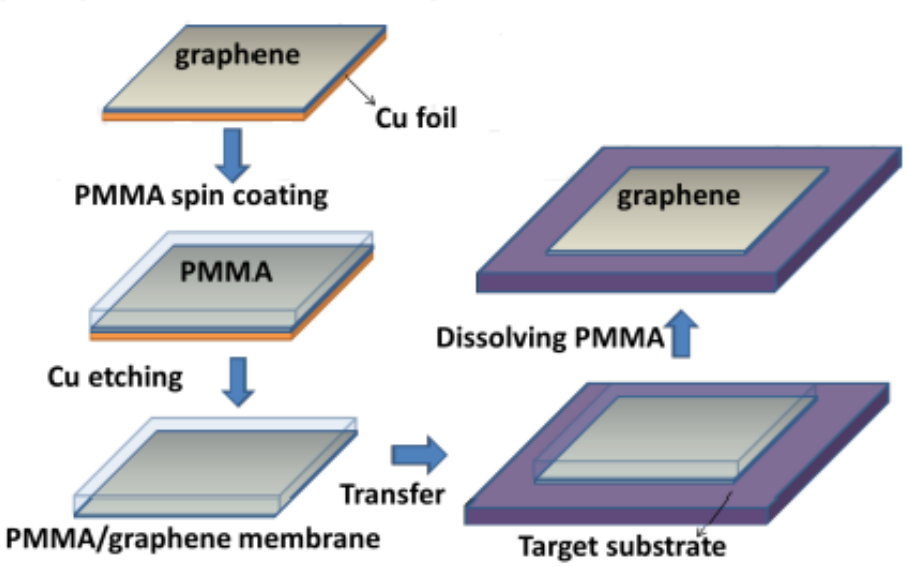

FIGURE 2.4: The procedure of CVD graphene transfer with PMMA. [35].

The process steps of a typical graphene sheet transfer are illustrated in Figure 2.4. At first the polymethylmethacrylate (PMMA) is spin-coated on the graphene. Afterwards the copper is etched away in suitable etching agent, e.g. solution of $Fe(NO_3)_3$ or $FeCl_3$. When the copper foil is dissolved, the graphene sheet is released and floats on the surface of the etching solution. PMMA acts as

a support structure for the graphene. This structure can be finally moved to the desired substrate. After the sample dries out the PMMA layer is dissolved with acetone or chloroform.

The transferring procedure is a delicate process and each step can introduce defects into the graphene layer. Furthermore it is extremely difficult to remove completely the PMMA layer on graphene. Usually a certain amount of impurities is left on the surface. Therefore an enormous effort is being made to find the proper transferring method which preserves the great graphene quality even after transferring. For this reasons additional process steps can apply such as PMMA heating, high vacuum annealing, oxygen plasma treatment or other special substrate treatment [35].

2.2 Characterization of Graphene

The characterization of graphene is a great issue. It is an interesting challenge to be able to sense one layer of atoms. Graphene is being studied such intensively that a fast and reliable characterization method is of a great importance. The method of choice for graphene characterization is a Raman spectroscopy. Even though that there had been done a lot of work done on characterizing graphene by various microscopy or spectroscopy techniques (XPS, SEM, TEM, STM, AFM), the Raman spectroscopy is still the most popular. The Raman process is complex but the technology of the measurement itself is fast, simple, non-destructive and it is capable to determine immediately the number of carbon layers on the surface. However its capabilities goes far beyond this knowledge. It is widely used for characterization of amorphous carbon, fullerens, nanotubes or diamonds. Particularly it is useful for graphene since the absence of a band gap makes all incident wavelengths resonant so that the Raman spectrum contains information about both atomic structure and electronic properties [36].

The principle of the method relies on inelastic scattering of monochromatic light, which is usually a laser in visible, near-infrared (NIV) or near-ultraviolet (NUV) range. The light which is coming back from the sample is then analyzed by spectrometer. The incident laser light interacts with the system of molecules in the sample. Most of the photons are scattered elastically which is an event known as Rayleigh scattering (see Figure 2.5). In contrast to Rayleigh scattering, the Raman scattering is typically a very weak phenomenon and therefore the wavelengths close to the laser line are filtered out. The impinging light interacts with the illuminated molecule and the photon excites the molecule from the ground state to the virtual excited state. Afterwards the molecule relaxes but not to the ground state but to the higher vibrational or rotational state. In consequence the photon is emitted at a different wavelength then the original initial photon. This leads to the shift of the wavelength which is called a Raman shift and it corresponds to the excitation energy of the molecule. If the frequency of the photon is shifted to a lower frequency and the final molecular state is higher in energy then the ground state, the shift is called Stokes shift. If the final molecular state is lower in energy then the initial state the emitted photon has a higher energy and this is denoted as an anti-Stokes shift (see Figure 2.5).

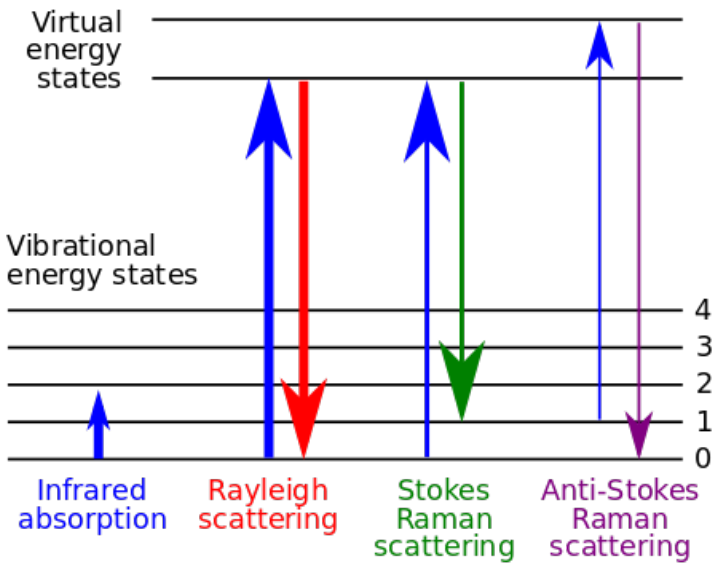

FIGURE 2.5: Energy-level diagram showing the states involved in a Raman signal. Image taken from [37].

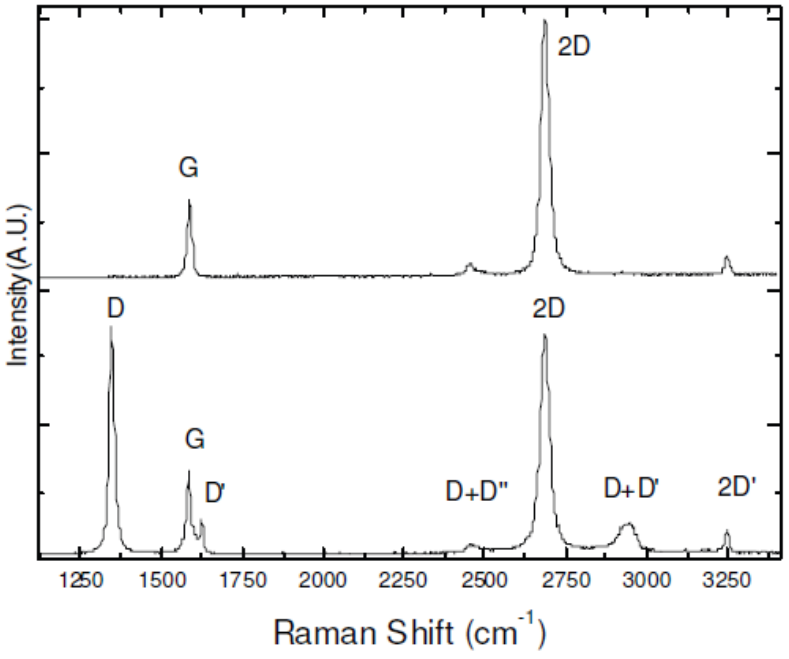

FIGURE 2.6: Top – Raman spectra of pristine graphene. In the spectrum only G and and 2D peaks are significant. Bottom – defected graphene. The spectrum has more significant peaks which are related to the distortions in graphene. Most significant of them is the D peak. Image taken from [36]

Raman spectrum of single layer graphene consists of distinct peaks (see Figure 2.6). These peaks are shifted from the laser wave number in the range c.a. $1200-3300\,\mathrm{cm}^{-1}$. The most important peaks for graphene characterization are 2D (c.a. $2700\,\mathrm{cm}^{-1}$) peak, G peak (c.a. $1582\,\mathrm{cm}^{-1}$) and D peak (c.a. $1350\,\mathrm{cm}^{-1}$). The G peak corresponds to a primary in-plane vibrational mode. The 2D peak is second-order overtone of a different in-plane vibration and the D peak is its first-order overtone [38]. Similarly the 2D' peak is the D' overtone. 2D and 2D' peaks originate from a process where momentum conservation is satisfied by two phonons with opposite wavevectors. The presence of any defects is not required for their activation and they are therefore always present in the Raman spectrum [36]. The D and D' peaks are symmetry-prohibited in ideal graphene and one can relate them to the level of disorder in graphene. If the structural defects are not present, the graphene is pristine and only 2D and G peaks are significant.

The spectrum of graphene is strongly changing with the graphene quality and with increasing number of graphene layers stacked. There is a significant change in the shape and intensity of the 2D peak when moving from SLG to graphite (see Figure 2.7). If the number of graphene layers is increasing the peak is being red-shifted. The G peak position is not changing that much with an increasing number of layers.

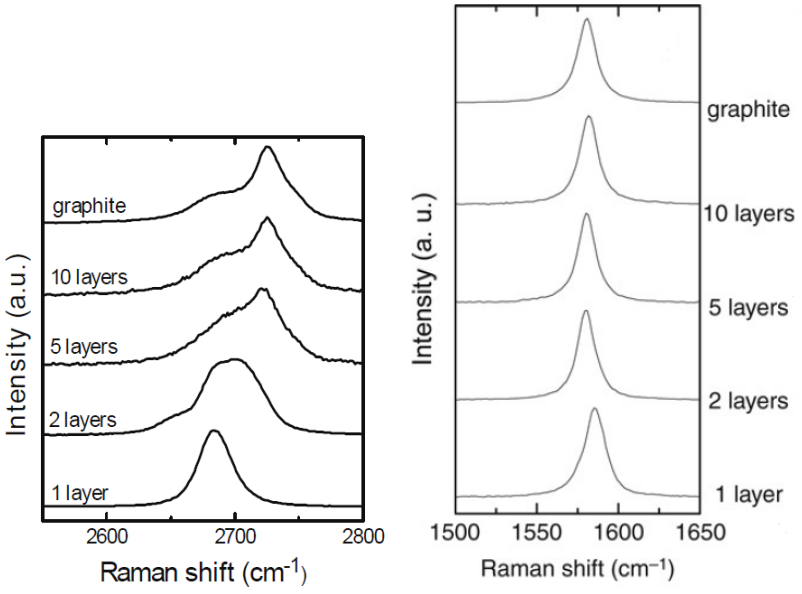

FIGURE 2.7: Left – 2D peak of graphenes Raman spectrum. The shape and position of it varies with increasing number of graphene layers [36]. Right – G peak of Raman spectrum, with increasing number of graphene layers it shows no significant shift [39].

A strong evidence of the presence of a single layer graphene on the surface is a ratio of 2D/G intensity (see Figure 2.8). In the case of pristine SLG the 2D/G ratio is c.a. 2. In the case of graphite, the G peak is more intense than the 2D peak and the 2D/G ratio is c.a. 0.5. The situation between these two extreme cases is difficult to examine. It was proved that if the thickness of graphene is increasing the 2D/G ratio is decreasing and in case of 2-layer graphene sample the

2D/G ration is c.a. 1. The determination of the exact number of the graphene layers in a multi layer graphene is extremely difficult and so far there is no specific evaluation method for this purpose.

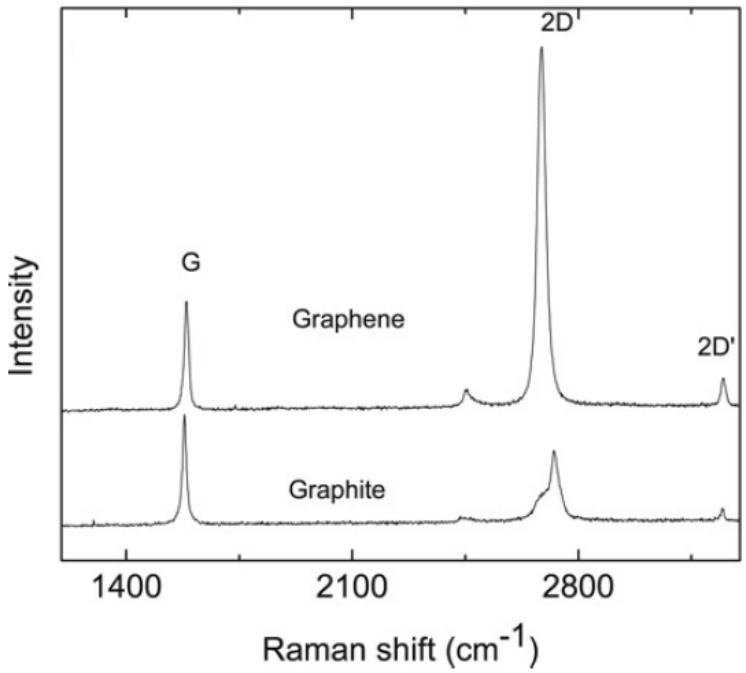

FIGURE 2.8: Top – Raman spectrum of pristine graphene. Bottom – Raman spectrum of graphite. With increasing number of graphene layers the 2D/G ratio is decreasing. For pristine graphene the 2D/G ratio is 0.5 [39].

3 Gallium and gallium nitride on graphene

This chapter describes the motivation for the study of gallium and gallium nitride properties on graphene. In the first part I will focus on the properties and interesting features of gallium on graphene. Later in the second part of this chapter I will discuss the features of GaN on graphene. I will focus also on the latest scientific achievements in these research fields. There is a colossal difference in behavior of gallium and gallium nitride. The first one is a metal and the second one is a semiconductor. They are both discussed in this work because the GaN preparation method is based on a creation of Ga structures followed by their nitridation. This is a unique advantage of our GaN preparation method – it is easily switching between metal and semiconductor material and therefore we are potentially able to watch the unique properties of these two materials together.

3.1 Gallium on graphene

Gallium is a metal and usually it forms small metallic spherical islands on the surface when deposited on a substrate. This depends on various deposition parameters – on the temperature and on the amount of material which is being deposited and on the substrate itself. If gallium is being deposited on graphene, the situation is similar and gallium is forming spheres on this surface as well. This was the initial part of my experimental work and I have been studying these samples. It is suitable to look for a parallel story in a modern research studies.

The relevant topic is the research of gold nanoparticles on graphene. Gold forms similar nanostructures on graphene and it is also a metal so it can possibly exhibit similar behavior. Even though various kinds of the nanoparticles were deposited on graphene (MnO_2, TiO_2, NiO, ZnO, Pt or Ag [40]) the gold still remains the most intensively studied material on graphene and the most similar to gallium.

The presence of metal nanoparticles on graphene can affect the electronic properties of graphene. Strong plasmonic effects can occur on the surface and they can possibly improve the performance of graphene-based devices. Metal nanoparticles can effectively dope the graphene's electronic system which can lead to the functionalization of graphene. In the case of gold nanoparticles (Au NPs) it was shown that Au NPs can be used to perform both p-type and n-type doping. This depends on the amount of gold deposited on the surface which determines the interaction between graphene and the different Au configurations (isolated

nanoparticles or continuous film) [42]. The chemical interaction between Au and graphene can also break the translational symmetry of the graphene lattice. This results in the presence of D band in the Raman spectra which is associated with a level of defects in the structure [43].

Surface-enhanced Raman scattering (SERS) is an important effect which is being studied mainly with gold nanoparticles on graphene. The effect involves surface plasmons which are induced by an incident field in the metallic nanostructures and increase the intensity of the Raman spectrum [36]. It was shown in many papers (e.g. in [41]) that the presence of the gold nanoparticles on the surface of graphene strongly increases the intensity of the whole Raman spectrum (see Figure 3.1 for details). The enhancement factor depends on the coverage and also on the size of the metal nanoparticles. In Figure 3.1 it can be seen that even with a low coverage of gold on the surface of graphene the enhancement factor was as high as 45. Similar results were reported on a number of graphene surfaces with different quality (mechanically exfoliated graphene or CVD graphene). Recently it was also shown that the gold nanoparticles can propagate through few-layer graphene [44]. This phenomenon implies that it is important to study the properties of the metal NPs on graphene to preserve its high electronic quality.

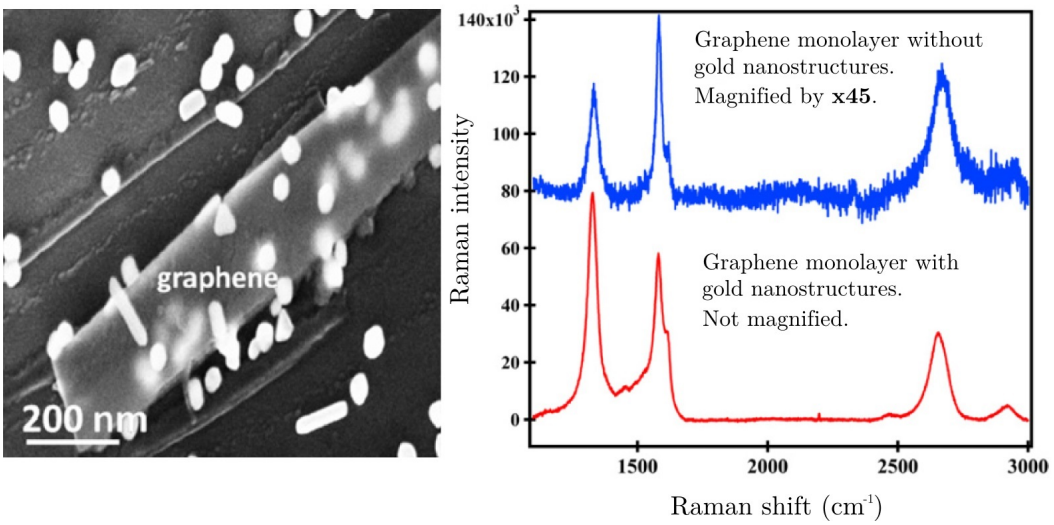

FIGURE 3.1: Left – SEM image of gold nanoparticles on graphene flake on Si with SiO_2. Right – Blue spectrum is a Raman spectrum of blank graphene sheet. The spectrum is magnified by 45. The red spectrum is a not-magnified Raman spectrum of graphene with gold nanoparticles. Images taken from [41].

The gallium nanoparticles on graphene have still not attracted such a wide attention like the research of the Au NPs on graphene. Recently it was shown in a theoretical study that gallium can effectively dope graphene and enhance the reactivity of graphene to H_2S gas sensing [45]. In this theoretical study a density functional theory (DFT) calculations are used to examine adsorption of H_2S on graphene. These calculations were made with boron, aluminum and gallium as dopant elements. The results indicate that the H_2S molecule binding to graphene is very weak in case of pure graphene and boron doped graphene with small adsorption values. The aluminum and gallium doped graphene have a large

adsorption energies and binding distances which are typical for the chemisorption. This implies that gallium can be effectively used for a graphene functionalization.

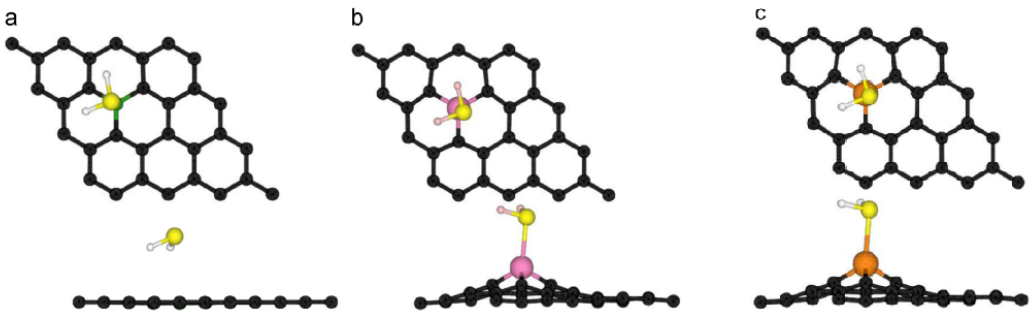

FIGURE 3.2: Left – The atom of boron which is incorporated into the graphene sheet. Middle – Silver dopant inside a graphene layer, forming a bond with H_2S. Right – Gallium dopant inside a graphene sheet, bonding with a H_2S, forming a bump in the flat layer. Image taken from [45].

In Figure 3.2 are illustrated the results of the DFT calculations. Boron dopant (Figure 3.2 a) does not change the planarity of the graphene sheet and after the adsorption of H_2S there is no significant change in the structure. In case of aluminum doped graphene (AG) and gallium doped graphene (GG), the planar structure of boron doped graphene (BG) is metastable and it is not achieved. In the ground state the structure forms a bump (see Figure 3.2(b,c)). The H_2S molecule is bound strongly after adsorption in case of AG and GG. It is important to point out that it is actually the local curvature of the graphene sheet which is responsible for the increased reactivity by causing higher strain in the doped system [45]. The boron atom has similar size as the carbon atom and therefore the final reconstruction corresponds to the pristine graphene. Furthermore, the interaction of gallium with graphene is predominantly ionic and with a weak bonding charge yielding minimal distortion of the graphene lattice [43]. Gallium and carbon are also insoluble which is another characteristics which makes gallium an important and functional material when related to graphene.

Really extensive work had been done very recently (published in February 2014) in [43]. In this work Losurdo's group is presenting a very wide research on the topic of gallium nanoparticles on the graphene sheets. They have used CVD graphene which was transferred onto the silicon substrate with 300 nm of SiO_2. For the gallium deposition, they have used molecular beam epitaxy system with the ultra high vacuum conditions. I have used similar procedure during my work on this project and the work of Losurdo's group was highly inspirational to me even though they have used much higher coverage of gallium on graphene and they have not presented data about Ga adsorption on the surface.

In Figure 3.3 there is a SEM image of a graphene completely coated with gallium spheres. Gallium exhibits this spherical growth all over the surface. Losurdo et al. have been studying the influence of gallium spheres on the graphene quality and therefore they have performed X-ray photoelectron spectroscopy (XPS) measurements in a graphene's valence band (see Figure 3.3). In this XPS valence band spectrum there are peaks related to graphene π bonding.

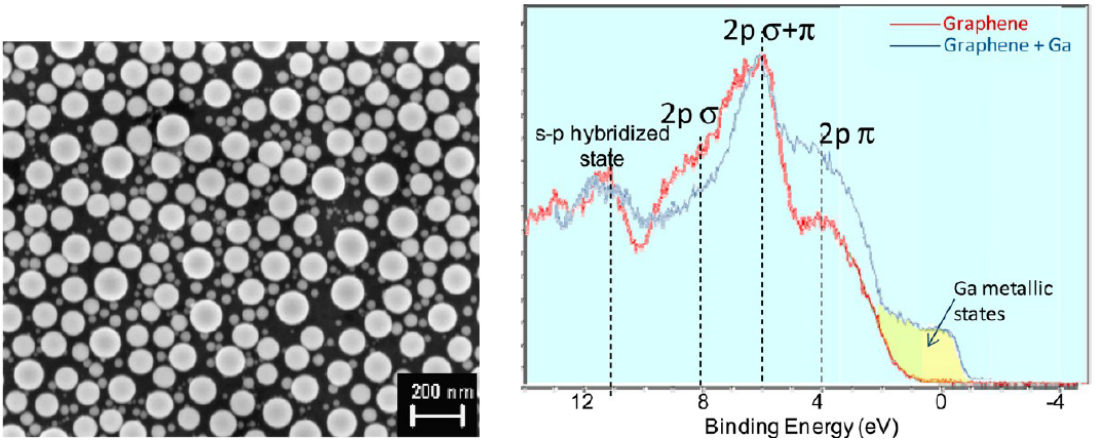

FIGURE 3.3: Left – SEM image of gallium nanoparticles on the graphene on SiO_2/Si. Right – XPS spectra of the valence band of graphene (red curve) and Ga NPs on graphene (blue curve). Taken from [43].

According to [46] the C 2p π is between 0 an 4 eV, crossing of C 2p π and C 2p σ around 6 eV, the C 2p σ at 7.9 eV, C 2s-2p hybridized state at 10.5 eV and C 2s σ band at 13.3 eV. The chemical bonding of a gallium atom to graphene requires a local rehybridization from sp^2 to sp^3 and this has a strong effect on the XPS valence band spectrum. Part of the 2p π states would be transformed into a C – Ga states and that would cause a decrease of the 2p π state with increasing Ga coverage [43]. After the deposition of gallium no increase of this peak occurs which implies that gallium does not rehybridize with graphene and the Ga NPs/-graphene interface has a high integrity. This is another feature of gallium which preserves the graphene structure.

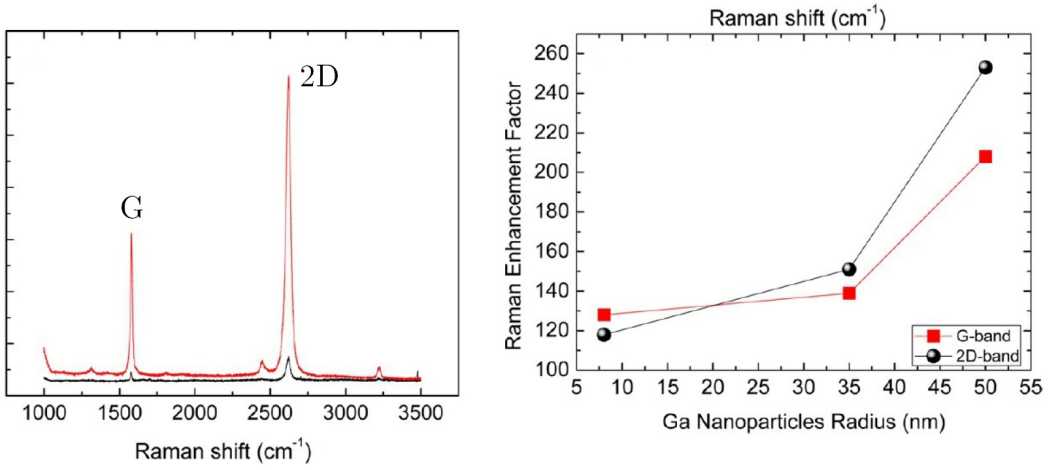

FIGURE 3.4: Left – Raman spectrum of graphene before (black) and after (red) deposition of Ga NPs. Right – Enhancement factor of the G and 2D peak which is dependent on a nanoparticle radius [43].

Losurdo's group has also presented SERS measurements of a gallium on graphene. Figure 3.4 shows the Raman spectrum of their samples after the gallium deposition. They show that the spectrum intensity increased and the enhancement

factor is in the range of several hundreds and also that it is dependent on the size of the gallium nanoparticles. I was observing this phenomenon as well during the experimental part of my thesis.

They have also shown Kelvin probe force microscopy (KPFM) measurements of the work function. The KPFM shows that the surface potential of graphene with Ga NPs increases by 150±50 mV which corresponds to a lower work function of graphene with gallium NPs as compared with the bare graphene [43]. See Figure 3.5 for details. The rest of their recent work was dealing with el-

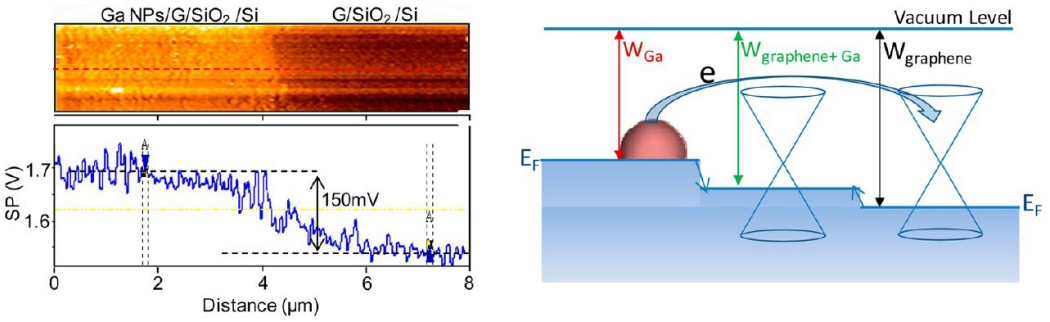

FIGURE 3.5: KPFM measurement of a boundary between graphene with Ga NPs and without Ga NPs. Left – surface potential measurement of such boundary. Right – Scheme of the work function values. [43].

lipsometry measurements of such surface and the paper has shown the importance and qualities of gallium/graphene interface. Their study triggered my interest in similar Raman spectroscopy and XPS measurements with different substrates and with a goal of performing similar experiments with a low coverage of gallium and possibly connecting this work to gallium nitride.

3.2 Gallium nitride on graphene

As mentioned earlier, GaN is a semiconductor material with exceptional properties which is widely used in high-power electronics and optoelectronics. The motivation for connecting GaN with graphene has therefore its industrial background.

A serious issue is the lack of suitable substrates for a growth of GaN devices. Most of the GaN devices are still being deposited on sapphire or silicon carbide. These substrates are highly expensive and there is still no substrate for effective, cheap, large scale growth of GaN even though there is a lot of papers about GaN growth on silicon or glass.

The growth of GaN on graphene has several advantages. Graphene films are stable at high-temperature, flexible, optically transparent, and have good electrical and thermal conductivity [47]. Furthermore, large-scale CVD graphene can be now relatively easily synthesized even though the transfer of the graphene is still problematic. GaN is traditionally used for LED fabrication. Therefore considerable scientific attention is given to this topic. Graphene can serve as a flexible transparent electrode which is an essential part of a novel LED displays. So far,

indium tin oxide (ITO) is used for these purposes. However, ITO suffers from relatively high price of indium and from its diffusion into the semiconductor's bulk. For these reasons it is an advantage to have an alternative transparent electrode with possibly better qualities [53]. Number of papers are published in this field and I will briefly discuss them later in this chapter. On the other hand, little attention was paid in the use of graphene as a substrate for GaN growth.

In 2009 a theoretical paper about GaN epitaxial growth on graphene [48] was published. The DFT calculations were performed to determine whether the epitaxial growth on graphene is possible or not.

The calculation has shown that the growth of GaN(0001) orientation on graphene sheet is possible even though the lattice mismatch is not low, but this is suppressed because the two-dimensional character of graphene which allows the strain relaxation. Thus graphene may be an ideal lattice mismatch free substrate for heteroepitaxial growth of materials with hexagonal symmetry (see Figure 3.6 for the calculated structure).

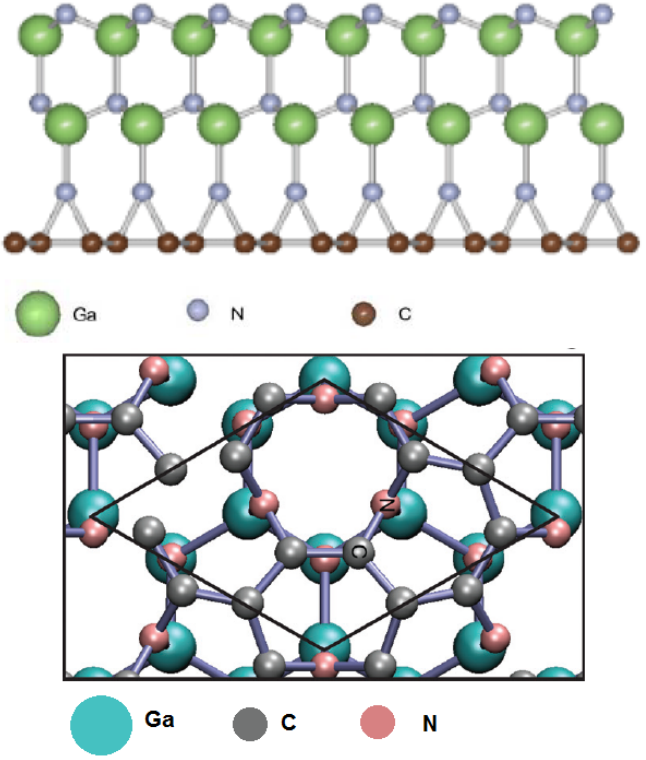

FIGURE 3.6: Top – The calculated results of the structure of the epitaxially grown N-terminated GaN(0001) on graphene [48]. Bottom – Optimized atomic structures of GaN-$\sqrt{3} \times \sqrt{3}$/graphene-2×2 superstructure [49].

Computational study [49] has shown GaN-$\sqrt{3} \times \sqrt{3}$/graphene-2×2 superstructure which is according to the paper the most probable and stable interface atomic structure. In this superstructure three C-C bonds of graphene are replaced with C-N-C bonds to stabilize the structure. In this case the GaN-graphene structure is nearly lattice matched. However, the interface structure is changing with the increasing amount of deposited GaN and the interface is strained. At a certain

point the strain is suddenly released by breaking part of the C-bond network and the structure is relaxed. See Figure 3.6 for the schematic of the superstructure.

Even though these theoretical studies show that stable GaN structures on graphene are possible, the direct growth of GaN on graphene is generally difficult. This is most likely due to the chemical inertness of graphene sheet. So far there are no studies concerning the MBE-grown GaN on graphene. All of the recent experimental studies are using the MOCVD method. The GaN growth in the experimental studies is performed with supporting structures (usually ZnO) or without them.

3.2.1 GaN growth on graphene without supporting structures

Ref. [51] reports on the deposition of GaN nanostructures on a few-layer graphene (FLG) using CVD method without any catalyst. The growth of GaN flower-like nanostructures on the FLG was observed (see Figure 3.7 for image). It was presumed that the growth is self-catalytic on FLG and is activated in the presence of an energy stored in the FLG surface. Large scale structures of GaN were obtained and these samples exhibited a distinctive photoluminescence (see Figure 3.7) even though the growth was not epitaxial.

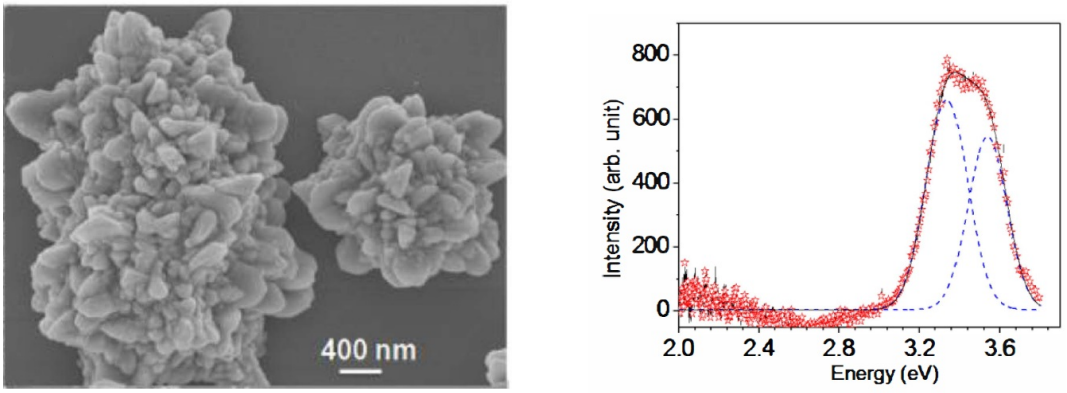

FIGURE 3.7: Left – GaN nanostructures obtained on few-layer graphene (FLG) sample. Right – Photoluminescence spectrum of these nanostructures. Images are taken from [51].

GaN films on graphene without supporting structures were also reported in [50]. As a substrate, sapphire coated by graphene was used. For the graphene coating a diffusion-assisted synthesis (DAS) method was used [50]. Graphene layer made by this method contains very rough multilayer sheet features which are creating ridges on the surface. GaN is afterwards nucleating along these ridges as demonstrated by a conventional MOCVD method. It was also concluded that the wettability between GaN and sapphire can be greatly altered by the insertion of a graphene sheet.

3.2.2 GaN growth on graphene with supporting structures

The growth with the supporting structures generally produces GaN layers of higher quality. Therefore there is a number of papers on this topic. In [47] conventional two-step MOCVD process (using a low-temperature GaN buffer layer) for a GaN nucleation on graphene was used. However, smooth GaN films were not obtained only a number of gallium droplets with a few GaN crystals and nanowires was observed on the surface. To improve the growth the paper presents the usage of a AlN buffer layer which was deposited on graphene. With the AlN buffer layer present the GaN growth became possible. GaN polycrystaline nanostructures on these substrates with a strong photoluminescence spectra and not-defected Raman spectra of graphene were reported in this paper (see Figure 3.8).

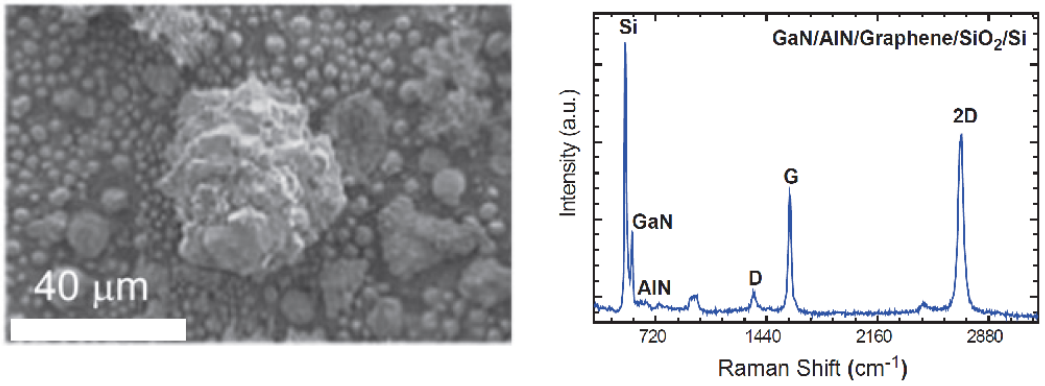

FIGURE 3.8: Left – GaN nanostructures obtained on AlN/graphene sample. Right – Raman spectrum showing distinct graphene peaks after the deposition of GaN [47].

Another option for the GaN growth is to use supporting ZnO nanostructures. The key for smooth GaN growth on graphene is a creation of step-edges on the graphene's surface. These step-edges can then act as nucleation sites. The creation of step-edges can be enhanced by treating the graphene samples in an oxygen plasma. However, the GaN growth on these samples still does not produce desired quality layers by conventional CVD methods and therefore high density ZnO nanowalls are grown on oxygen-plasma-treated graphene. The ZnO structures are grown by MOCVD method using diethylzinc (DEZn) and they nucleate along graphene's step-edges. GaN growth is afterwards realized as an epitaxial lateral overgrowth because ZnO has the same crystal structure and small lattice mismatch [52]. See Figure 3.9 for the growth steps.

So far this method has the biggest success in the production of high quality GaN layers on graphene and therefore it was recently used for LED fabrication. The motivation is obvious, graphene is suitable as a flexible transparent electrode. Ref. [52] reports the fabrication of a highly efficient LED on CVD graphene which was transferred onto silicon. This whole LED device was further transferred onto various substrates (plastics, glass, metal). Similar work had been successfully done in Ref. [54] as well.

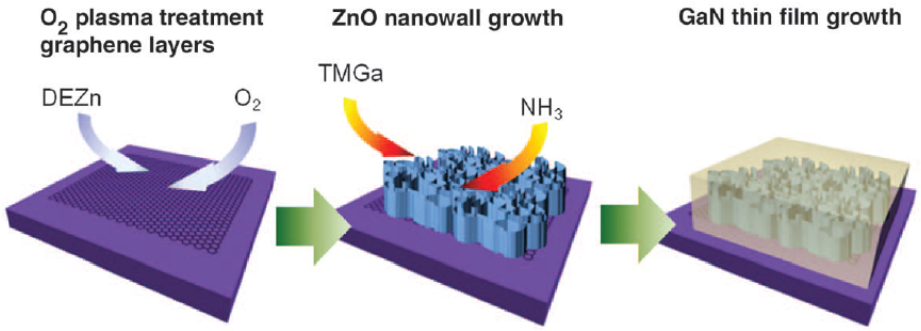

FIGURE 3.9: Process of GaN growth on graphene with ZnO nanowalls [52]. At first the ZnO nanowalls are grown and afterwards GaN is grown by MOCVD from TMGa and NH_3.

Ref. [55] reports on GaN microdisk arrays selectively grown on a silicon oxide using micropatterned graphene dots. The authors have used CVD graphene which was transfered on SiO_2/Si substrate. The graphene sheet was afterwards patterned using an electron beam lithography with a negative resist. The resist was used as an etch mask and the surrounding graphene was etched away by oxygen plasma forming regular graphene arrays (see Figure 3.10).

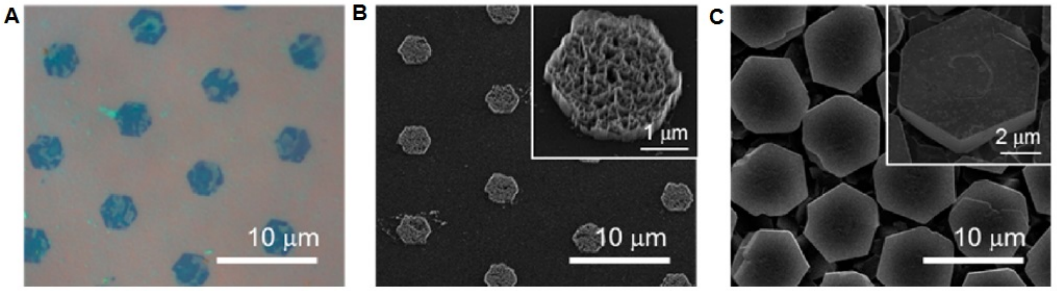

FIGURE 3.10: (a) Optical microscopic image of patterned graphene films after etching. (b) SEM image of graphene array with ZnO nanowalls. (c) SEM image of a GaN microdisk array after deposition of GaN [55].

Afterwards the ZnO nanostructures were deposited using the MOCVD method. In the last step the GaN microdisks were grown using conventional MOCVD two-step process by epitaxial lateral overgrowth of ZnO nanostructures. See Figure 3.10 for results. The final structure was an array of GaN disks which is very suitable for the fabrication of complex devices, including microdisk lasers. This is the first published successful attempt of a GaN selective growth on a graphene sheet.

4 | CVD graphene deposition

I will introduce the sample preparation method which was used for the preparation of the graphene samples and I will discuss the quality of the obtained graphene. This will be illustrated by the experiments. In chapters 5 and 6 I will discuss the Ga and GaN deposition on these samples. For these purposes it is extremely important to obtain insight into the properties of the graphene substrates. The experimental part of this work continues, confirms, extends and specifies the previous work which was done by Ing. Martin Dvořák. [56].

4.1 Preparation of CVD graphene samples

CVD graphene was prepared in a conventional apparatus which was built at the Institute of Physical Engineering by Pavel Procházka [34]. The deposition took place in a furnace made from quartz glass which is heated by a resistive-heating wire. A clean 25 μm-thick copper foil samples were inserted into the furnace. The furnace was afterwards pumped with a turbomolecular pump and a rotary vane pump.

First step of the deposition procedure was annealing of the copper foils at 1000 °C for 25 minutes in a hydrogen atmosphere with a pressure $p = 5.4$ Pa and a hydrogen mass flow $f_{\mathrm{H2}} = 2$ sccm. The pressure was measured by a Pirani gauge and the hydrogen mass flow was measured by a mass flow controller (MFC) valve.

In the second step the graphene growth occurs. Two different structures can be obtained after this step – graphene polycrystals (large graphene sheet) or graphene monocrystals. Polycrystalline graphene sheets were obtained with the following setting. After the annealing the methane was introduced into the furnace with a flow $f_{\mathrm{CH4}} = 2$ sccm at 1000 °C and with the hydrogen flow f_{H2}=2 sccm and the pressure was then set to p=67 Pa. The deposition of graphene then took 30 minutes with this settings. Afterwards the samples were cooled down and taken out of the furnace. This procedure results in a large graphene sheet on the copper foil. The graphene grows as a grain on various nucleation sites on the surface. These grains grow until they merge together and form a graphene layer.

Monocrystalline graphene was then obtained just by decreasing the deposition pressure to p=16 Pa alongside with keeping the rest of the parameters constant. This results in a slower growth of the graphene flakes and the grains do not merge together so a surface with individual graphene grains is obtained. The graphene quality is kept the same, only on a smaller area. Similar result would

be achieved if all the parameters were kept constant and only the deposition time decreased.

Monocrystalline graphene which was deposited in the furnace is shown in Figure 4.1. The scanning electron microscope (SEM) image shows graphene flakes which cover the copper foil. The graphene is not visible in SEM so only the clean copper foil with stripes from rolling underneath the graphene sheet can be seen. The flake is surrounded by an area of copper which is oxidized and therefore the graphene flake is visible.

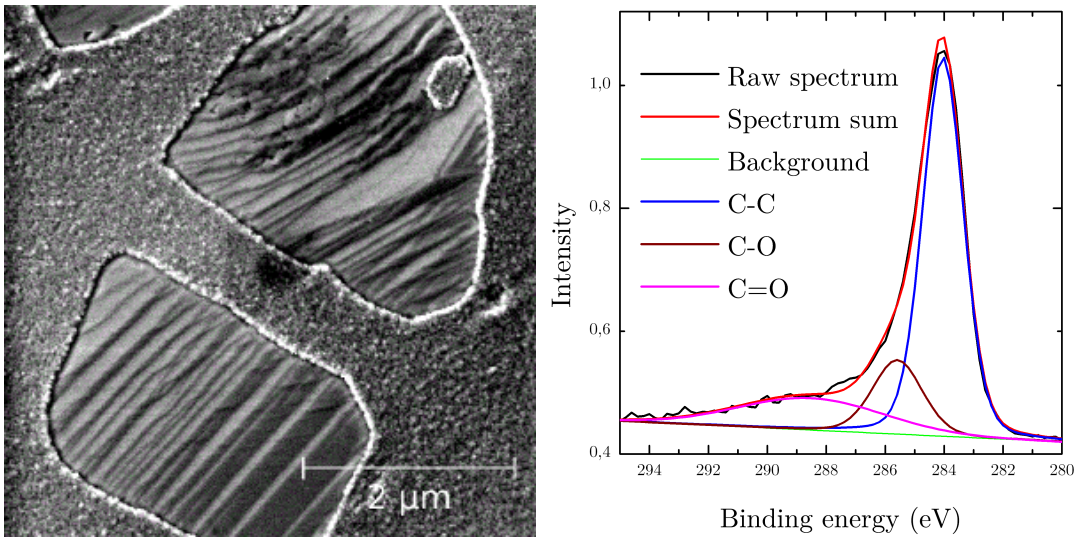

FIGURE 4.1: Left – SEM image of a monocrystalline graphene on a copper foil. A clean copper foil is covered by two graphene flakes and the oxidized copper is providing a visible border. Right – XPS measurement of the C 1s peak of graphene on copper foil with a characteristic asymmetric shape.

The quality of the graphene layer on a copper foil is supposed to be excellent if no impurities are involved in the deposition system. The evaluation of the graphene quality is crucial for the following experiments. I have inspected this by measuring the Raman spectrum of the graphene samples. The Raman spectrum of the graphene monocrystals on a copper foil is shown in Figure 4.3.

The Raman spectrum was obtained with a green laser (523 nm) with a 10 s acquisition time. There is a really strong photoluminescence in this region which is related to the Cu foil. The complete interpretation of this spectrum is therefore difficult. I have fitted the broad photoluminescence peak by Gaussian function and then subtracted it from the measured Raman spectrum. The result is in the Figure 4.3. Only the 2D and G peak are present in the Raman spectrum. The 2D peak is c.a. two times more intense then the G peak which confirms the presence of a monolayer graphene sheet. There was no indication of the D peak in the spectrum which confirms that there are no distortions in the graphene and the graphene is pristine. The rest of the distinct peaks are related with a copper substrate. Similar results were obtained on most of the samples.

I have also studied the X-ray photoelectron spectroscopy (XPS) spectrum of these samples. XPS is a basic analytical method in surface science. It can

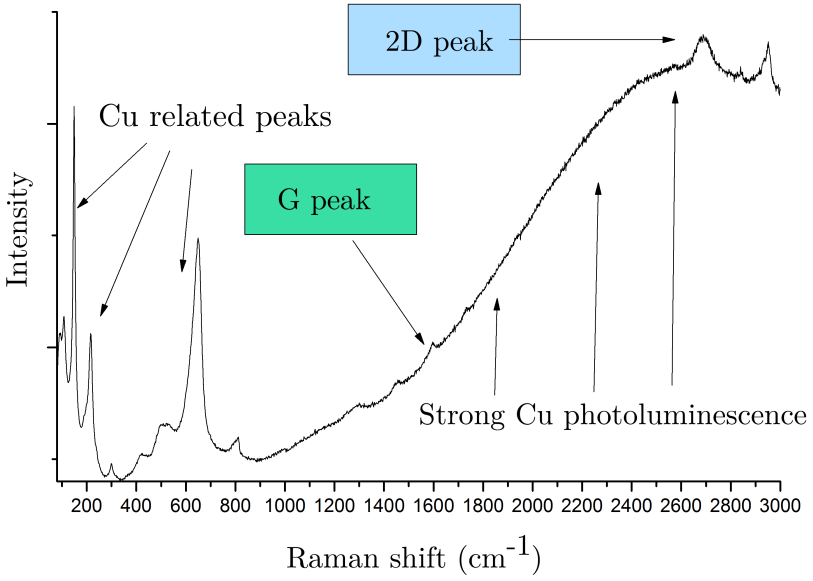

FIGURE 4.2: Raman spectrum of a graphene flake on a copper foil. There is a strong Cu photoluminescence, other Cu related peaks and 2D and G carbon peaks.

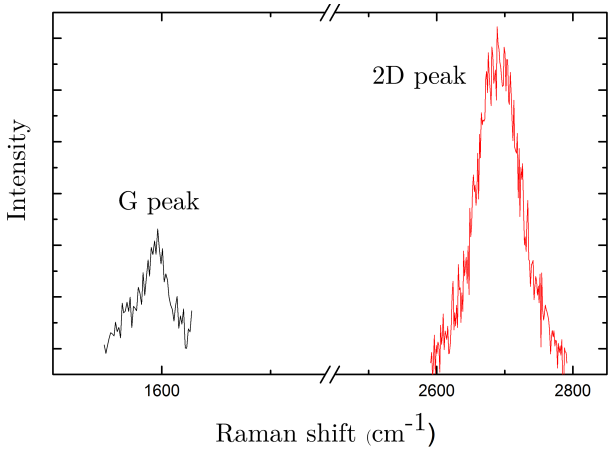

FIGURE 4.3: Carbon peaks of a Raman spectrum of a single graphene flake on copper foil. 2D/G ratio is 2 which corresponds to the pristine graphene.

be used only in high vacuum conditions (pressure $< 5{\cdot}10^{-6}$ Pa). It uses an X-ray source which provides a well defined characteristic X-ray beam. Usually the Al Kα(1486.7 eV) or Mg Kα(1253.6 eV) characteristic X-ray lines are used. The analyzed surface is irradiated by this radiation. The incoming photons penetrate into the surface to the depth of several micrometers and in consequence the surface emits electrons from a depth of several nanometers. This happens because X-ray photons can be absorbed by the atoms of the substrate and the photon energy can be given to the core level electrons of the atoms. These electrons are then emitted from the surface with a specific amount of kinetic energy. Their kinetic energy is the difference between the energy of the incoming photon and the binding energy

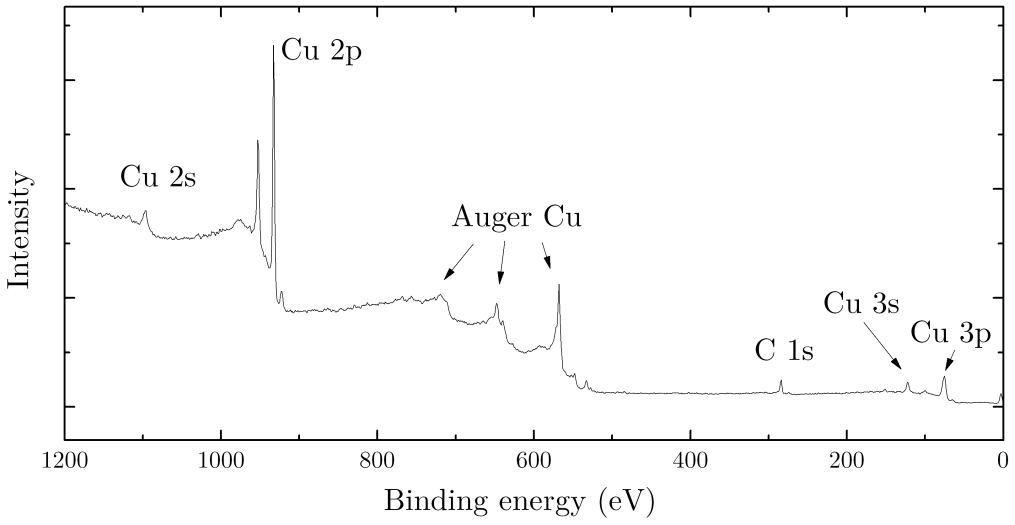

FIGURE 4.4: XPS spectrum of a copper foil with a CVD-deposited graphene sheet. Only the copper and carbon peaks occur in the spectrum which is demanded.

of an electron in the atomic structure and the work function of the spectrometer. This allows to determine the binding energy of the electrons. The emitted electrons are analyzed by a hemispherical analyzer which measures the distribution of the kinetic energy of the emitted electrons. The final spectrum shows the number of emitted electrons as a function of their kinetic energy (and consequently the binding energy). The spectrum shows distinct peaks which belong to the core-level electrons of the analyzed element. XPS is also chemically sensitive. If the analyzed element is chemically bonded to a different element the binding energy of its electrons will change and in the XPS another peak occurs with a slight chemical shift (several eV).

The XPS spectrum of a copper foil with graphene is shown in the Figure 4.4. Prior to the measurement, the sample was annealed in the UHV at 400 °C for 180 minutes to desorb copper oxide, water and other atmospheric adsorbates. Afterwards the XPS measurement was performed. The spectrum shows only distinct peaks of copper and carbon. This indicates that no significant impurities are present on the surface. I have focused on a C 1s peak of carbon. In the case of graphene the C 1s peak should have an broad asymmetric shape towards the higher binding energy which indicates sp^2 carbon structure. This is confirmed also for our samples (see Figure 4.1) where the C 1s peak has such asymmetry. Because the asymmetrical tail can originate from the functionalization of graphene by oxide I have fitted the spectra with the parameters from [57]. The exact interpretation is not straightforward but definitely the spectrum implies that the majority of the carbon on the surface is composed of sp^2 carbon and therefore the structure is

graphene-like. Together with the conclusions from the Raman measurements and from the SEM images it can be concluded that the graphene is of an excellent quality after the deposition on the copper foil.

4.2 CVD graphene transfer

Graphene transfer was a crucial step of the sample preparation. A conventional method with polymethylmetacrylate (PMMA) spincoating was used to transfer the graphene. This method was chosen because so far it is the most reliable method providing sufficient results. The procedure was divided into several steps. For a schematic of the procedure see Figure 2.4. At first PMMA was spin coated on the top of the graphene layer on copper foil. PMMA created a support structure for the graphene sheet. In the next step the samples were treated by oxygen plasma to remove graphene from the other side of the copper foil. Afterwards the Cu foil was etched away. For this step a solution of $Fe(NO_3)_3{\cdot}9H_2O$ with a concentration $0.05\,g{\cdot}ml^{-1}$ was used. In the next step the graphene with PMMA was transfered on the water surface where it was cleaned from the etching solution. The structure on the water surface was then moved to the desired substrate where it was dried out. In the last step the PMMA was removed which was done by inserting the sample into acetone for 12 hours.

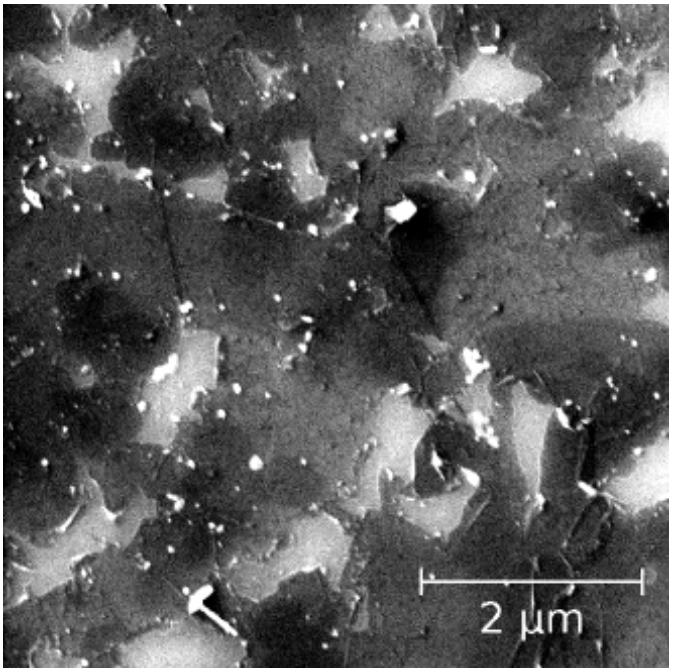

FIGURE 4.5: SEM image of a polycrystalline large graphene sheet after the transfer. High amount of distortions was introduced during the transfer. The bright small areas correspond to the underlying SiO_2 substrate. The transferred graphene sheet is displayed by darker areas.

Large polycrystaline graphene sheet after the transfer is shown in the Figure 4.5. A high amount of distortions and cracks is observed in the SEM image. These were introduced mechanically during the transfer.

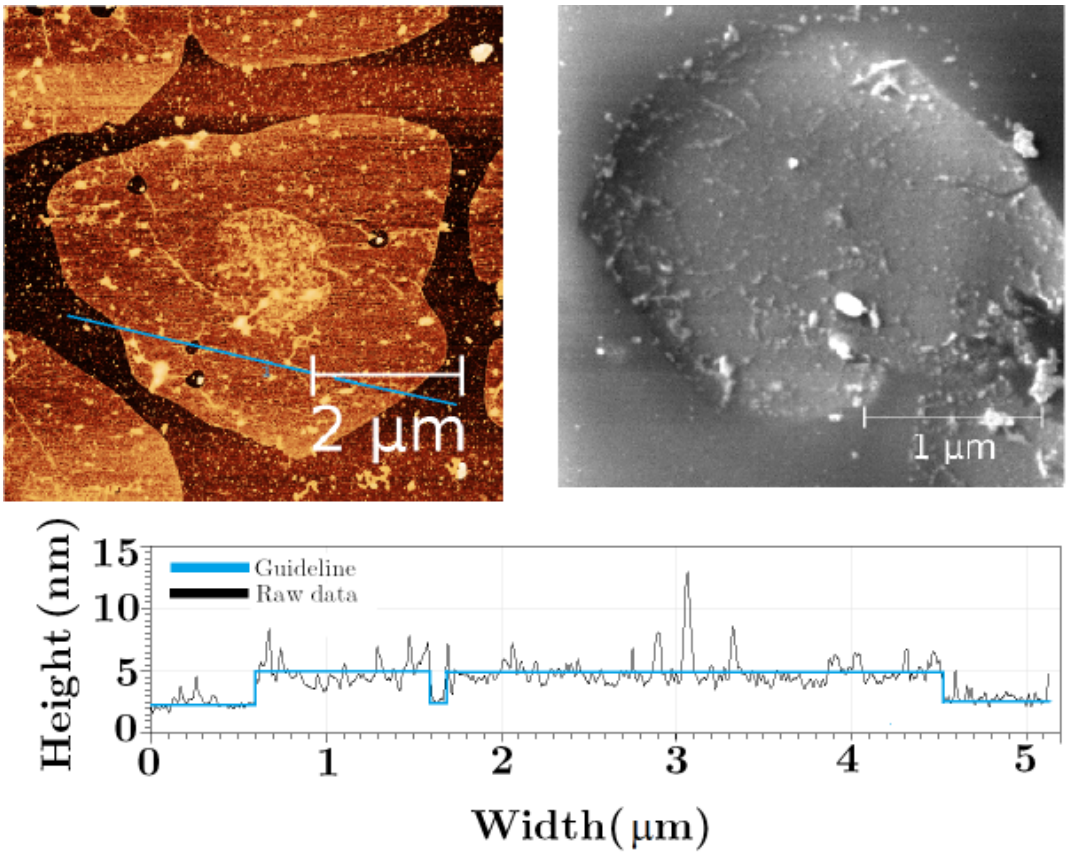

FIGURE 4.6: AFM image of a transferred graphene flake with a linear profile of the height. SEM image of similar graphene flake. Most of the impurities on the graphene sheet are the PMMA residues.

Graphene flakes after the transfer are shown in Figure 4.6. SEM and atomic force microscopy (AFM) measurements of these samples were done to reveal the structure of the transferred graphene sheets. From the images it is obvious that after the transfer many features can be observed on the graphene sheets. The features are residues of PMMA which have remained on the surface due to an imperfect etching during the transfer. This is the property of the transfer method and still one of the biggest difficulties of a CVD graphene transfer. From the AFM measurements it can be seen that the graphene flakes are several nanometers in height. This indicates that there is a very thin layer of PMMA residues which is creating a rough structured layer on top of the graphene sheet.

I have used two different types of the substrates for the graphene transfer. A silicon substrate Si(111) with native SiO_2 (N-doped with resistivity of 0.029 – 0.03 Ωm and a silicon Si(100) with 280 nm of SiO_2 (N-doped with resistivity of 0.0014 Ωm). For Ga and GaN growth on graphene, there is no significant difference between both substrates as shown in the following chapters. However, the thickness of the SiO_2 effects greatly the further graphene characterization by Raman spectroscopy. The 280 nm layer of SiO_2 was chosen due to exceptional optical properties which are significantly enhancing the intensity of the Raman peaks by the multiple reflections on the Si/SiO_2 multilayer. The magnitude of the interference effect depends on the thickness of the SiO_2 layer and on the laser wavelenght

(see Figure 4.7). The enhancement factor of the carbon peaks is furthermore different for each peak [58].

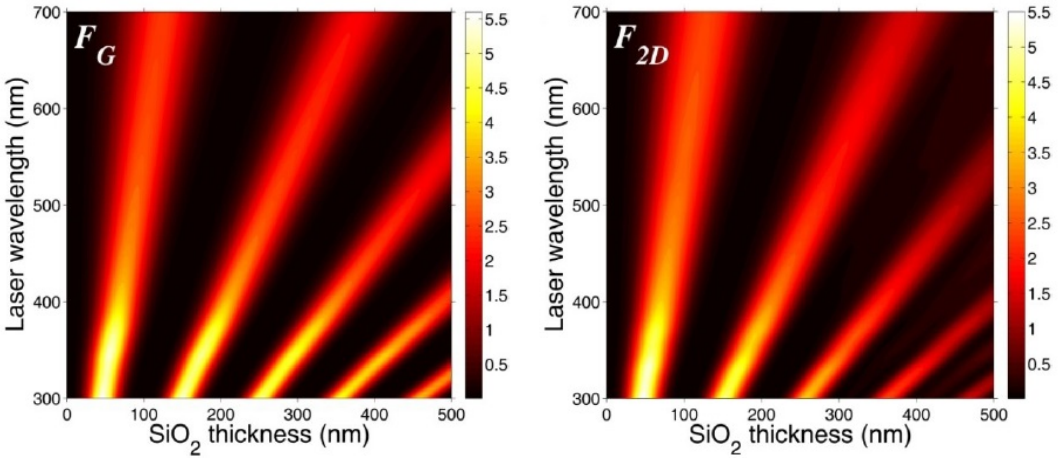

FIGURE 4.7: Plot of the calculated Raman enhancement factors (F) of the G band and 2D band as a function of the thickness of the SiO_2 layer and the laser wavelength [58].

This has a strong effect on the intensity of the Raman spectrum and also on the 2D/G ratio which is different for the same graphene sheet on different substrates and thus the 2D/G ratio is 2 only for pristine graphene on 280 nm SiO_2. These measurements are illustrated in the Figure 4.8. Both spectra were normalized to the silicon second overtone peak in the Raman spectrum. In this spectrum the two identical sheets with graphene flakes were transferred onto two different substrates. The graph shows that the Raman spectrum intensity is significantly larger for the sample with 280 nm SiO_2 compared to the sample with native SiO_2. Furthermore the ratios of these peaks have slightly changed. From the 2D/G ratio of the black spectrum it can be assumed that there is more than one monolayer of carbon on the surface. The D peak is also present in the spectra which implies that there are distortions in the graphene's structure. This is strongly related to the PMMA residues on the top of graphene. However, the impact of these residues on the graphene quality is not fatal because the spectrum has not changed that significantly from the spectrum of pristine graphene.

I have also analyzed the transferred graphene sheets by XPS to see whether the C 1s peak has changed from the previous XPS measurements on a copper foil. At first I have annealed the samples in UHV conditions at 400 °C for at least 120 min. This is an important step for further depositions. The impurities which are adsorbed from atmosphere (water and organic impurities) are desorbed away by this step. Another advantage of the annealing is that the sample will get rid of part of the organic residues which come from PMMA. This was shown in [56]. After the annealing step the XPS measurements were performed. In Figure 4.9 XPS spectrum of an annealed graphene sheet on a 280 nm of SiO_2 is presented. The wide XPS spectrum shows only several noticeable peaks which were expected – silicon, carbon and oxygen. The C 1s peak is also similar to the C 1s peak of the pristine graphene. It has also an asymmetric shape towards the higher binding energies. I have also fitted the C 1s peak with known peak profiles of the

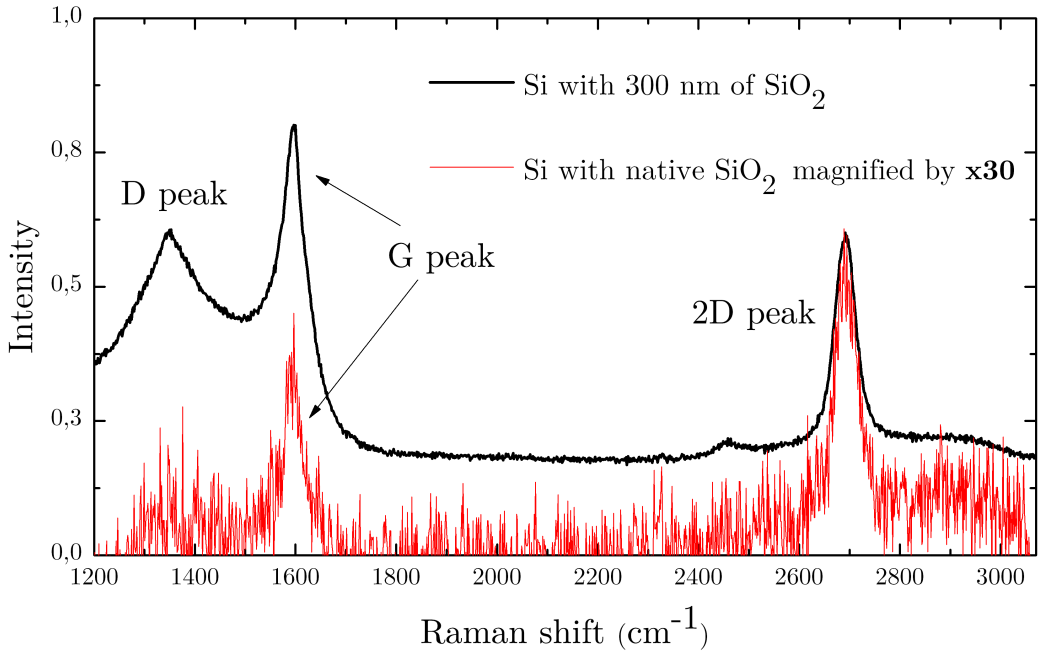

FIGURE 4.8: Raman spectrum of graphene which was transferred on a Si with native SiO_2 and Si with 280 nm of SiO_2. The red spectrum was magnified 30 times.

other possible carbon states on the surface (apart from the C-C chemical state) which could possibly occur in these samples. The C 1s spectrum of the transferred graphene is very similar to the C 1s spectrum of the graphene on a copper foil.

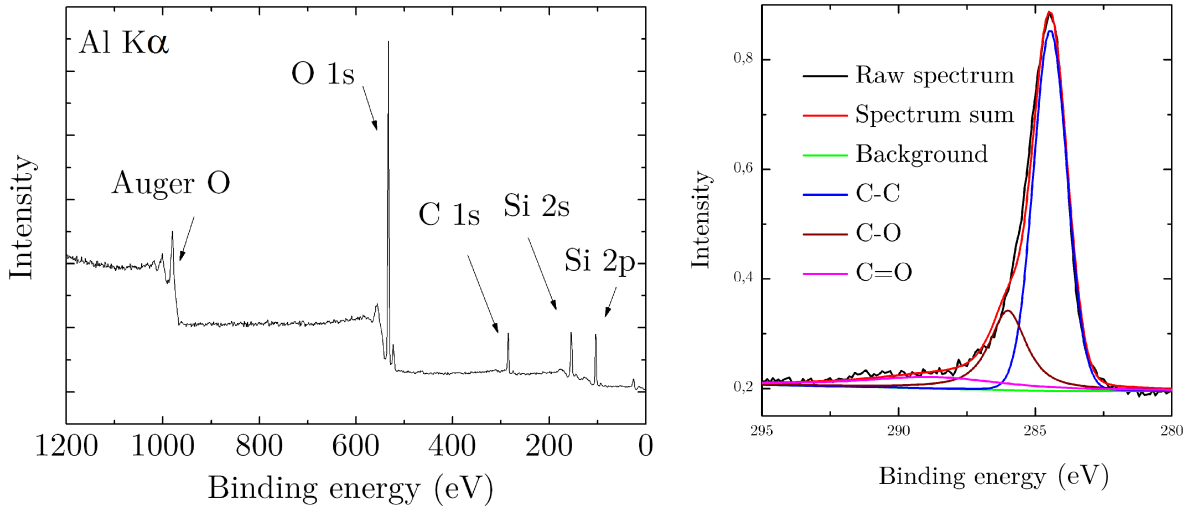

FIGURE 4.9: Left – XPS spectrum of graphene sheet after the transfer on the SiO_2. Right – C 1s XPS peak of the transferred graphene sheet.

From the AFM, SEM, XPS and Raman spectroscopy data it can be concluded that the graphene quality after the transfer is not excellent. It can

be also concluded that the PMMA residues are creating a rough surface. This is expressed in the Raman spectrum that differs from that of pristine graphene even though the changes are minor. However, the PMMA layer on the samples is still relatively thin, most likely with small areas of pristine graphene in them. Also the XPS spectrum of graphene was preserved after the graphene sheet transfer. The understanding of the surface properties is crucial for the next chapter. It will be shown that the adsorption properties of gallium are strongly related to the graphene sheet quality. Nevertheless, the prepared samples contain a graphene sheet and they can be used as substrates for the deposition of Ga and GaN.

5 Deposition of Ga on graphene sheets

All the experiments were performed in a complex UHV apparatus at the Institute of Physical Engineering (see Figure 5.1). The UHV complex consists of four chambers and a small load-lock. We have used two of the chambers – the deposition chamber and the analysis chamber. The base pressure in the deposition chamber during my experimental work was $1{\cdot}10^{-7}$ Pa. The base pressure in the analysis chamber was $2{\cdot}10^{-7}$ Pa and the pressure was measured by nitrogen calibrated Bayard-Alpert ionization gauge. To achieve this pressure the deposition chamber was pumped with a scroll pump followed by turbomolecular pump. In the analysis chamber a ion pump is used to achieve a sufficient UHV pressure.

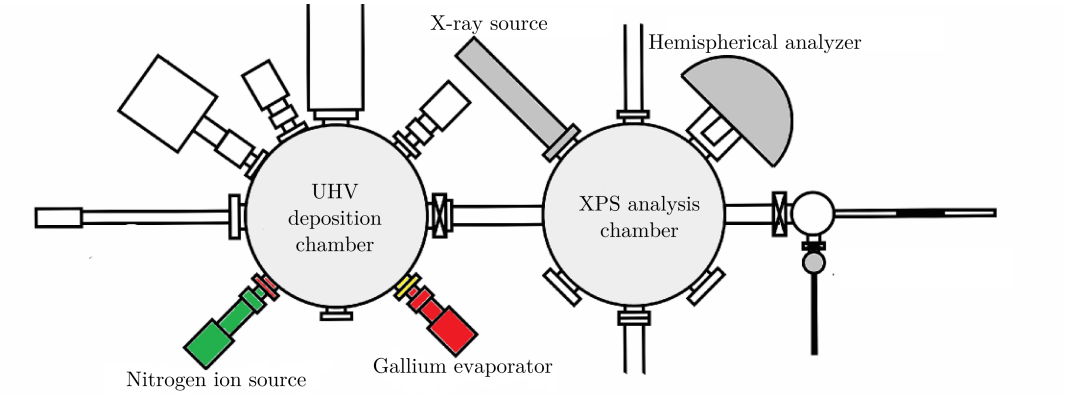

FIGURE 5.1: Scheme of a complex UHV apparatus consisting of deposition chamber and analysis chamber.

In the deposition chamber the effusion cell is used for the evaporation of gallium. It is a widely-used EFM-3 evaporator from the Omicron company. See Figure 5.2 for the schematics of the evaporator.

A molybdenum crucible filled with 99.9999% Ga metal was installed into the evaporator. The evaporation starts with a voltage (up to 1000 V) which is applied between the crucible and a tungsten wire. Tungsten wire is then heated by a current to a high temperature (c.a. 2800 K) where the thermal electron emmission starts. The whole tungsten wire is a cathode creating a source of electrons. The electrons are afterwards accelerated towards the crucible and they are hitting it. Due to this effect the crucible is heated. The temperature of the crucible (and the gallium inside) is thus governed by the magnitude of the current which is passing through the tungsten wire. This provides a precise balancing of the evaporant

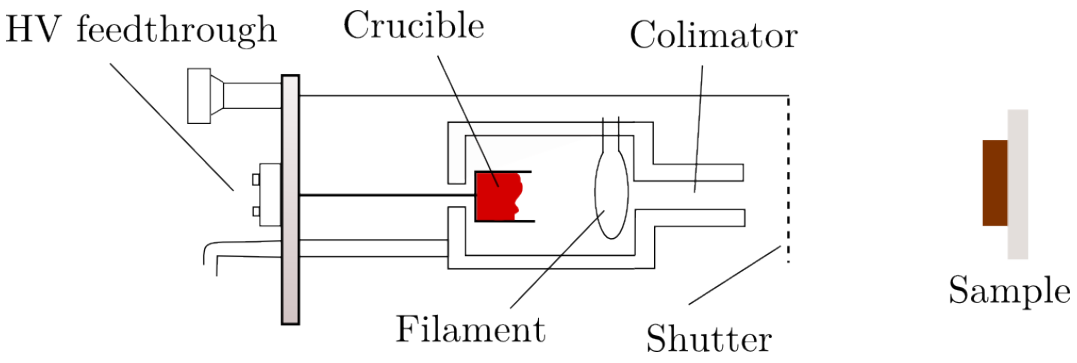

FIGURE 5.2: Schematics of the evaporator which was used for gallium depositions.

temperature. When gallium is heated enough to achieve the temperature c.a. 800 °C, the evaporation starts. Because of such a high temperature, the body of the evaporator is water-cooled. An atomic beam is passing through the collimator towards the sample. The deposition speed is governed by the Ga temperature. Some of the Ga atoms are ionized when passing through the collimator and this provides a current (in the range of nA) which is then measured as a flux and it corresponds to the actual amount of gallium in the deposition beam.

X-ray photoelectron spectroscopy (XPS) instrument is installed in the analysis chamber and it was routinely used for the basic characterization of the samples. The entryway for the samples is a small load-lock where the samples are inserted from the atmospheric pressure and then they are transfered by a system of magnetic rods to the desired deposition or analysis position.

5.1 Gallium deposition on CVD graphene on copper foil

I have made a series of Ga deposition experiments. Main goal was to analyze the behavior of an evaporated gallium after hitting the surface of the transferred graphene. The central element of all the surface events is the temperature. Therefore I have focused on the gallium deposition on graphene sheets at various temperatures. After inserting the sample in ultra-high vacuum conditions the samples were annealed at 400 °C overnight. The temperature was measured with an optical pyrometer (emissivity = 0.7). The accuracy of an optical pyrometer is low and the exact temperature values are not known precisely. However the temperature range I have used in the experiments is quite high and therefore the order of the temperatures (from low to high) can be secured. Samples were annealed for the reasons mentioned above. The annealing enables the desorbing of the atmospheric adsorbates and furthermore it allows to get rid of part of the PMMA residues and it is also lowers the average roughness of the graphene sheet which is crucial to prepare the surface for Ga deposition.

After the annealing the deposition of Ga from the evaporator has started. All the depositions were performed in a pressure lower than $3.4 \cdot 10^{-7}$ Pa. The deposition speed was controlled by the gallium flux which was measured on the

collimator of the evaporator. For all the depositions I used the same value of the flux corresponding to a current of 80 nA. This deposition speed is c.a. 0.2 ML/min. This flux was usually obtained with a 800 V acceleration voltage and with 32 mA emission current of the evaporator. The flux was kept stable during the deposition process.

At first I have made a series of depositions of Ga at various temperatures – room temperature, 200 °C, 300 °C, 350 °C, 400 °C, and 500 °C – on graphene sheets on a native SiO_2 and on 280 nm SiO_2. The Ga deposition time for these experiments was 60 minutes which corresponds to the 12 ML of Ga. After the deposition, the samples were analyzed by XPS, AFM, SEM, and Raman spectroscopy instruments.

The SEM measurements of the samples are shown in Figure 5.3. The samples in Figure 5.3 with the deposition temperature RT, 200 °C, 400°C and 500°C contain large graphene polycrystalline sheets. The samples with the temperature 300 °C and 350°C contain monocrystalline flakes of graphene. Only the 350°C sample is deposited on the 280 nm SiO_2 and the rest of the samples is deposited on Si(111) with native SiO_2. No difference in growth on these two substrates was noted in the later experiments.

The deposited gallium forms two types of structures on the surface – the gallium spheres and the gallium planes. I will first discuss the properties of the Ga spheres (droplets). The size of the spheres is increasing with the deposition temperature. This is due to the increasing diffusion length of gallium on the surface. I have analyzed the size of the spheres by the SEM and AFM measurements. The AFM measurements in Figure 5.4 reveals also the height information about the deposited structures. I have analyzed the SEM measurements to get the dependence of the average width of the spheres on temperature. The result is in Figure 5.5.

The graph shows that the average width of the spheres is increasing with the temperature and it is in range of 30 – 100 nm. At the 500 °C and at higher deposition temperature the gallium structures were not observed. Above this temperature all the impinging gallium atoms desorb from the surface. At lower temperature the Ga atoms are diffusing on the surface until they nucleate or until they merge with a Ga island.

I have compared the average width of the Ga spheres on the transferred CVD graphene with the width of the Ga spheres on Si/SiO_2 on the same substrate. This was possible because the graphene sheet covers only minor part of the whole SiO_2 substrate and the rest of the sample is only the Ga/SiO_2 interface. The black curve in Figure 5.5 shows the temperature dependence of the width of the Ga spheres on the SiO_2. The dependence is also increasing. It can be concluded from the graph that the diffusion length of Ga on graphene is higher then the diffusion length of Ga on SiO_2 in the measured temperature range.

The other features which are observed on the surface are the gallium planes. These features have lower height than the Ga spheres (see Figure 5.4 (c)) and they are usually much wider (hundreds of nanometers). In the SEM measurements they appear gray because they are thinner and therefore providing lower yield of secondary electrons.

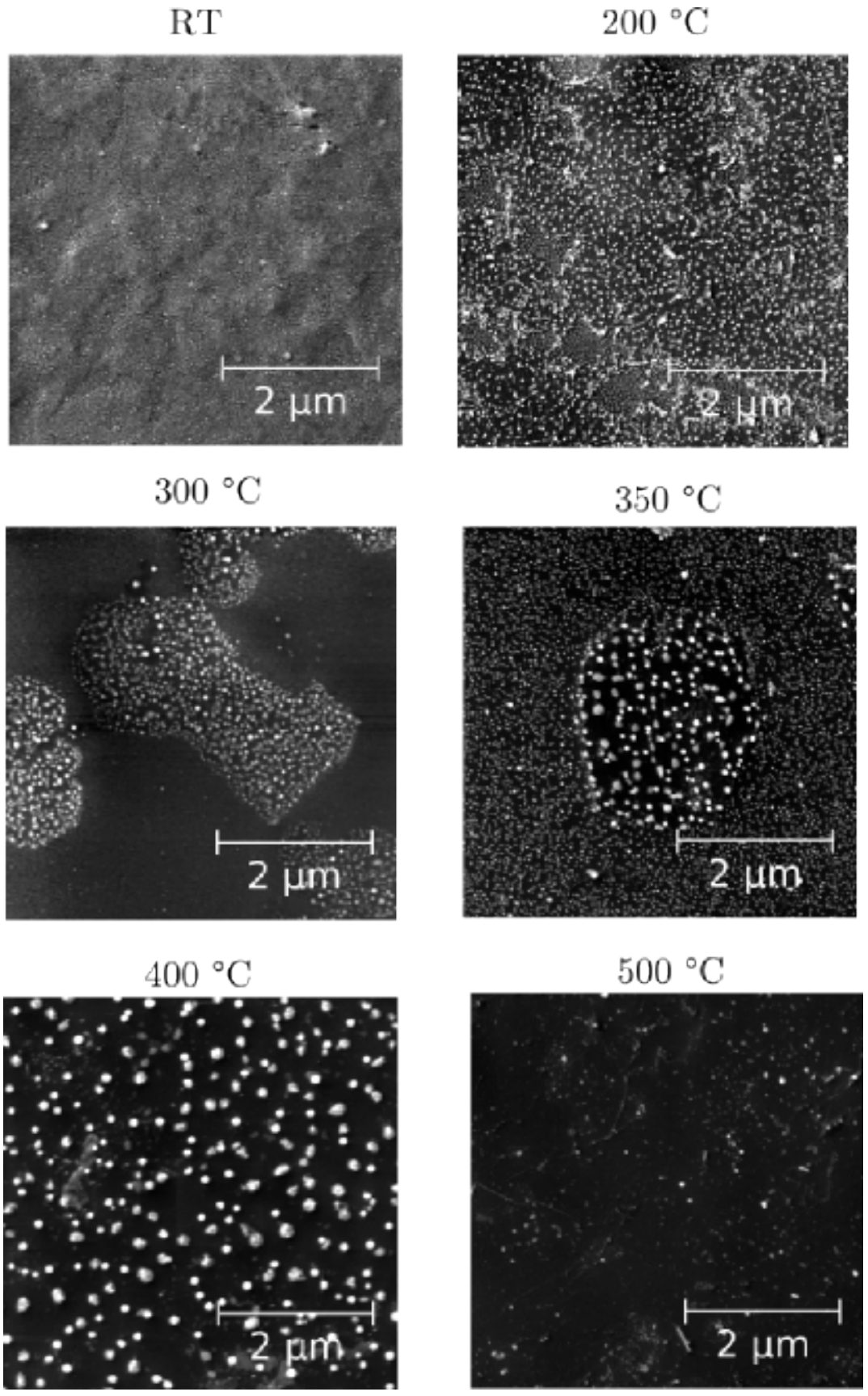

FIGURE 5.3: SEM images of the the deposition of Ga on graphene sheets at various temperatures. Deposition rate c.a. 0.2 ML/min, growth time = 60 minutes.

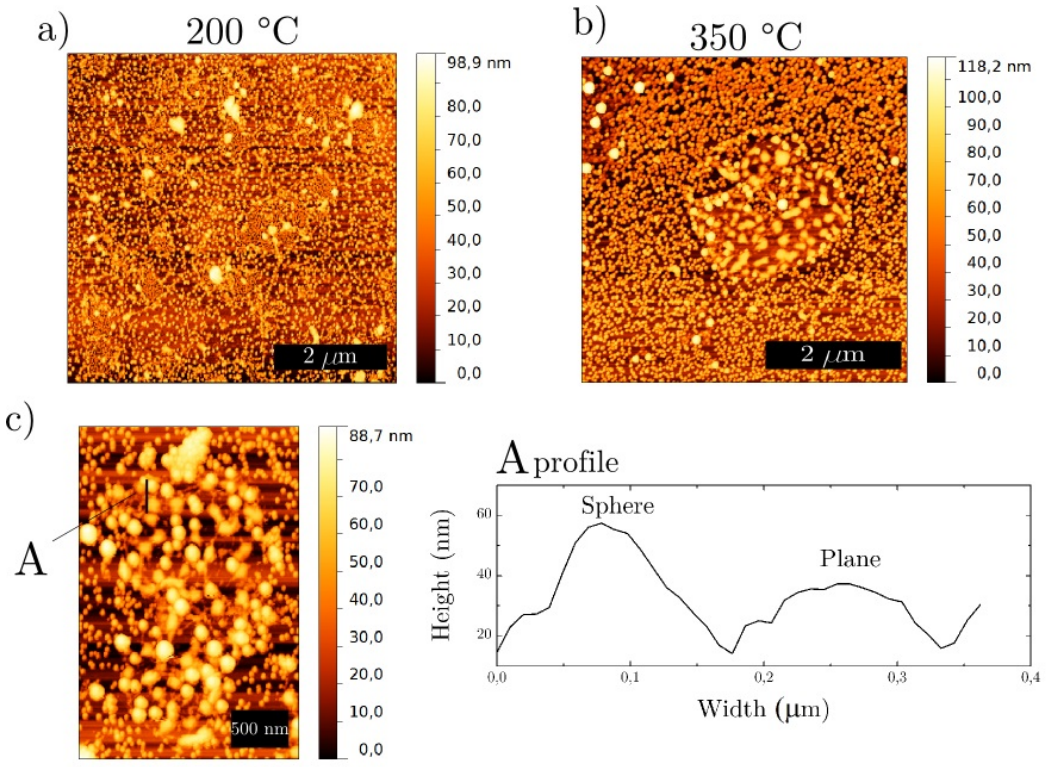

FIGURE 5.4: AFM measurements of the samples with deposited Ga. a) The measurement of the 200 °C sample. b) The AFM image of a graphene flake with deposited Ga at 350 °C. c) AFM detail of a flake on a 350 °C substrate which shows the difference between the Ga spheres and Ga planes.

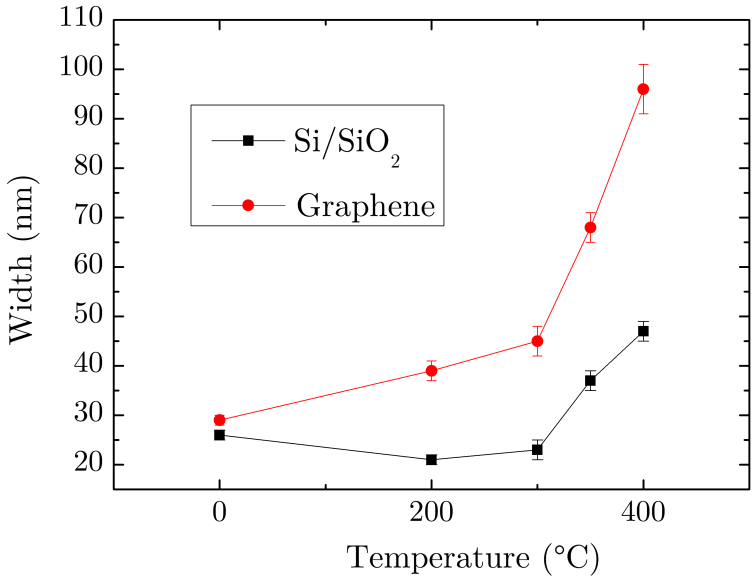

FIGURE 5.5: The dependence of the width of the Ga spheres and the temperature. This was measured for Si/SiO_2 substrate and for the graphene substrate. The data are connected by line for illustration.

At first it was not clear whether these structures are made from gallium. For this reason an energy-dispersive X-ray spectroscopy(EDX) measurements were made. EDX takes place in an electron microscope and it uses an X-ray analyzer to determine the energy of the photons emitted from the sample irradiated by an electron beam. The X-ray photons have a characteristic energy which corresponds to the core-level bands of the analyzed material and the EDX analyzer is able to measure the relative number of photons with a certain energy. The resulting spectrum is a dependence of the the intensity on the photon energy. It shows distinct peaks which are connected to the elements which are present on the surface. A great advantage of this method is that it is able to characterize the structure of the few-nanometer scale areas.

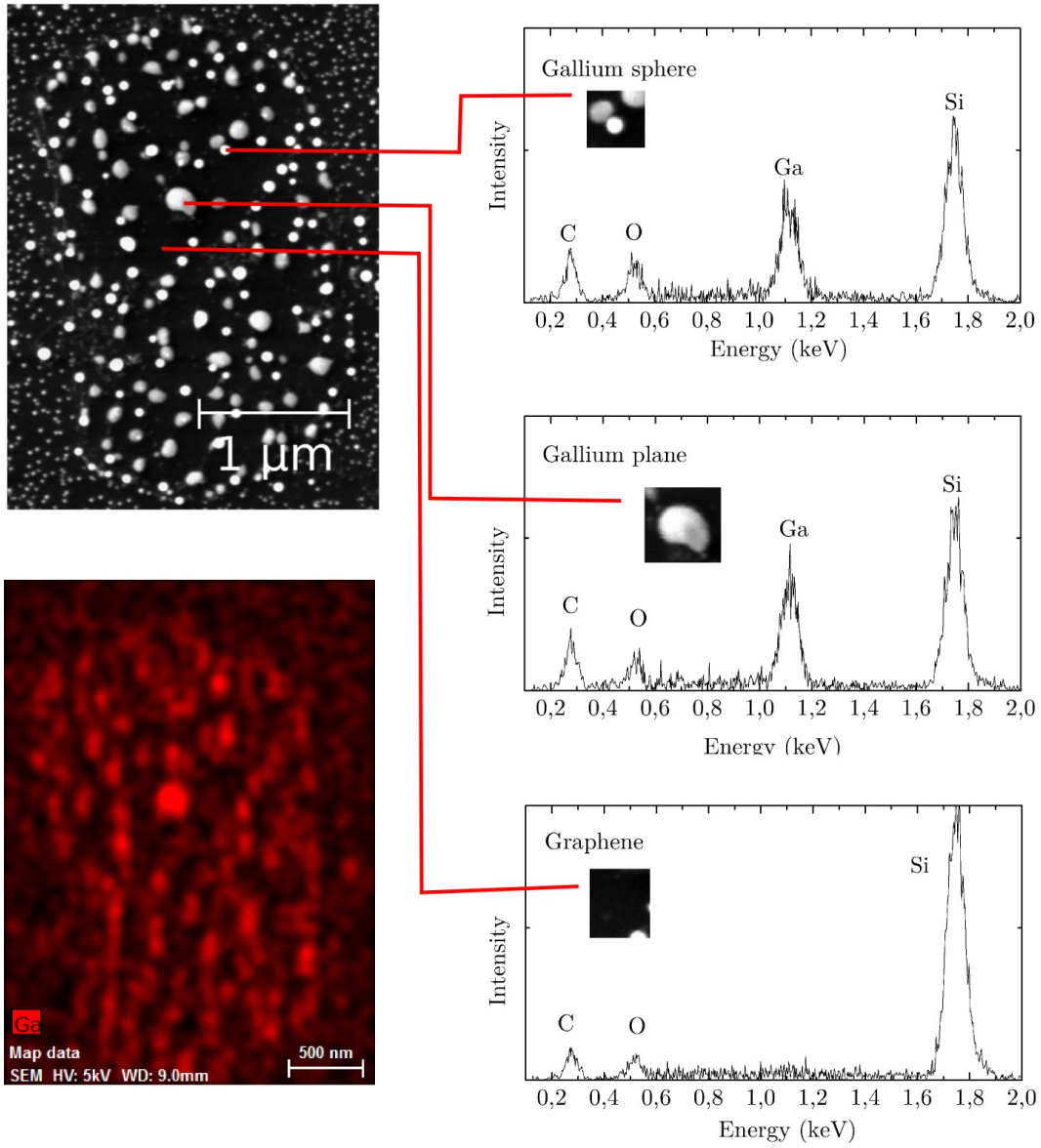

FIGURE 5.6: Top left panel: SEM image of a flake with deposited Ga. Right: Three EDX spectra from the 350 °C sample from various areas of the graphene flake. Bottom left panel: EDX map of the flake showing an incidence of the Ga Lα peak in the spectra.

The results of EDX measurements are shown in Figure 5.6. The data were measured on a graphene flake with Ga deposited at 350 °C for 60 min. There are three EDX spectra shown. The first spectrum was taken on one of the gallium spheres. The second spectrum was taken on one of the gallium planes and the last spectrum was taken on a place on the graphene sheet where no other feature was observed so it is assumed to be a clean graphene. From the measurement it is obvious that both the sphere feature and the plane feature contain gallium. The measured peak is Ga Lα (1.098 keV).

In addition to Ga, the Si, O and C peaks are present in the spectrum. These peaks are expected because they are related to the substrate. The high intensity carbon peak comes from the graphene, PMMA residues, and from the adsorbed atmospheric carbon. The bottom left panel shows a spatial distribution of the Ga Lα peak intensity over the sample (as obtained by EDX). The places with an intense Ga peak exactly correspond with the positions of Ga spheres and planes. For these reasons the measurements state that both the spheres and the planes are made from gallium.

The mechanism of the growth of the Ga planes is still not known exactly. The planes are not observed at the room temperature and hence the formation of the planes is related to a higher temperature. The two types of growth suggest that the surface is not homogeneous. The most probable scenario is that the transferred graphene on the SiO_2 layer has a number of distortions and impurities. These impurities locally change the wetting properties of the surface leading to a different type of Ga formation. This theory is supported by the density of the Ga planes because it is not constant over the sample. On several parts of the sample the density of the Ga planes is significantly lower than than on the other parts. In Figure 5.7 there are two different graphene flakes on the 350 °C sample with different density of the Ga planes. This also indicates that the two-type growth is connected to the substrate quality and not of the graphene substrate itself. On the right image in Figure 5.7 there is a higher amount of planes together with a higher amount of the impurities on the surface. This was observed on variety of substrates. The growth of the planes can be therefore connected with an inhomogeneous etching of the PMMA and with the impurities on the graphene. This theory will by also supported by the data presented in the following text.

A typical XPS spectrum of the deposited samples is shown in Figure 5.8. This is the spectrum of the graphene sheet where gallium was deposited at the room temperature. It shows that there are only expected peaks related to the substrate (Si, O, C) and peaks related to gallium. The intensities of peaks which are related to the substrate are low because at the RT the whole surface is covered by gallium.

5.2 Raman spectroscopy of Ga on graphene

The Raman signal of a sample can be strongly enhanced when the surface of the sample is covered by a thin metallic layer or metallic nanoparticles. We have performed Raman spectroscopy to study this effect for our Ga structures. As mentioned earlier the intensity and shape of the Raman spectrum depends on

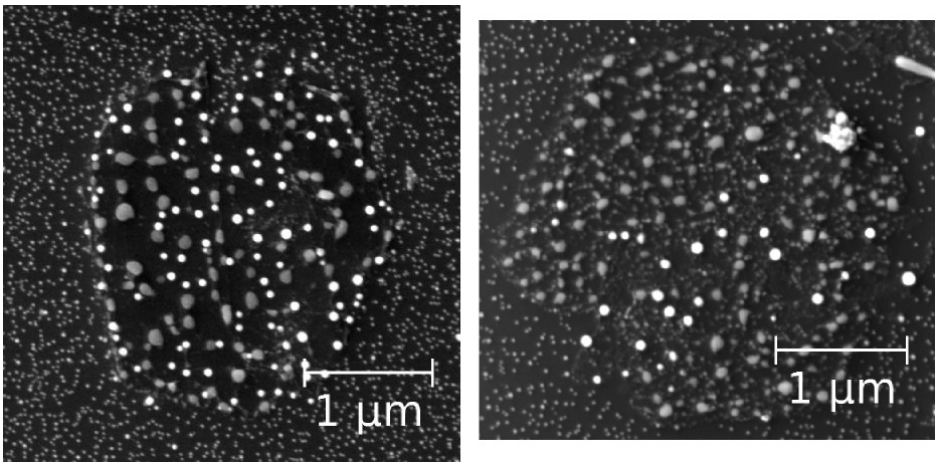

FIGURE 5.7: SEM images of two flakes at different parts of the 350 °C sample. The flake on the right contains relatively high amount of Ga planes (gray patches).

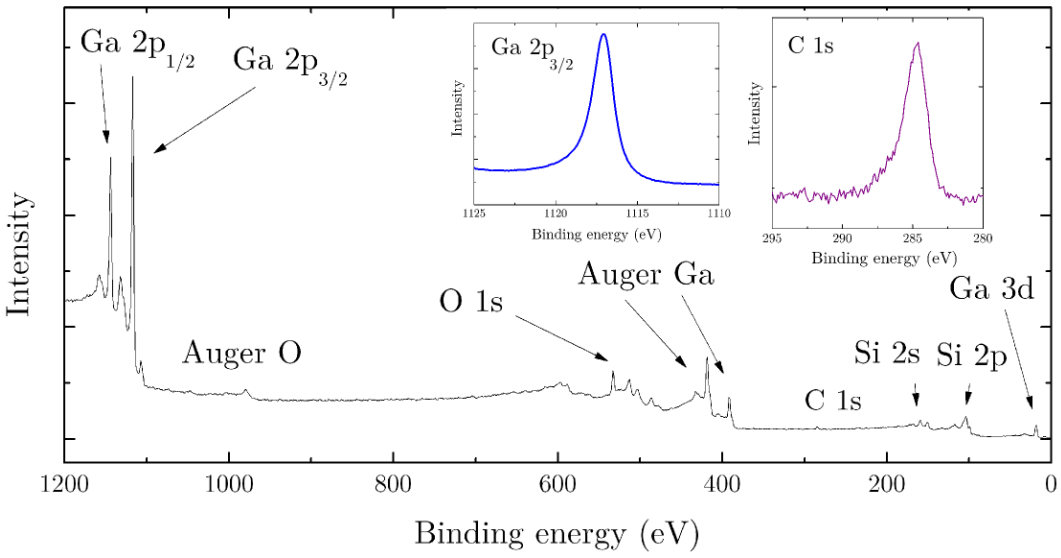

FIGURE 5.8: Wide XPS spectrum of the sample where Ga was deposited for 60 min at RT. The detail shows gallium Ga $2p_{3/2}$ band and C 1s band.

the used substrate. In Figure 5.9 the Raman spectroscopy graphs of the graphene substrates with gallium on the silicon with native SiO_2 are shown. The spectra show the range where carbon peaks occur. The data were normalized to the second order overtone of silicon and afterwards the spectrum obtained from the silicon background was subtracted. The data thus belongs only to the layer of Ga/-graphene. The black curve shows the spectrum of a clean graphene sheet without gallium. The rest of the curves show the spectrum obtained on the graphene sheet after the deposition of Ga for 1 hour with a deposition rate of 0.2 ML at room temperature, 200 °C, 350 °C, and 400 °C.

The intensity of the D, G and 2D peak increased with the deposition

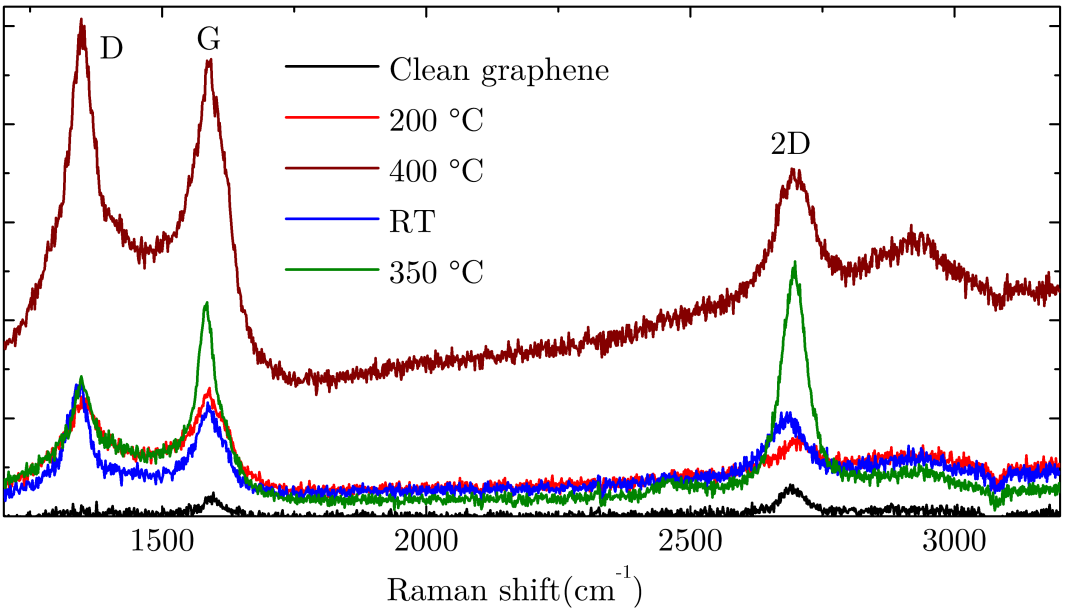

FIGURE 5.9: Raman spectra of the carbon peaks of the samples with the deposited gallium on Si(111) with native SiO_2. The spectra were normalized to the silicon's second order overtone and the silicon background was subtracted. The spectrum was measured with a green 523 nm laser.

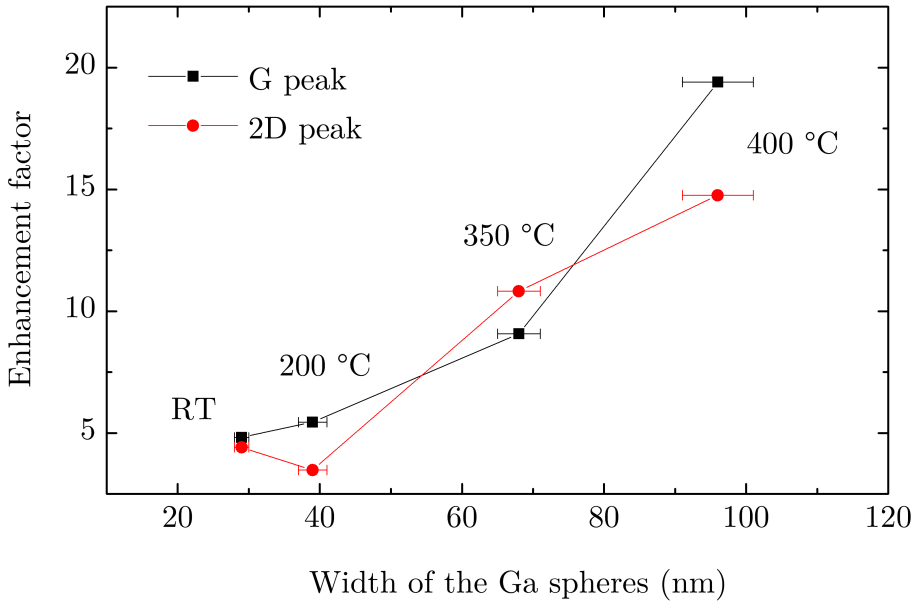

FIGURE 5.10: The enhancement factor of G and 2D peak as a dependence on the average width of the Ga spheres. The data are connected by line for illustration.

of Ga on the graphene sheet. Before the deposition of Ga the D peak was indistinct but afterwards its magnitude is comparable to the magnitude of the G peak. This means that the gallium adds to the graphene/Ga system a number of distortions. In general the intensity of the whole spectrum increased strongly. The Ga spheres on the surface caused a surface-enhanced Raman spectroscopy effect. The enhancement factor of this effect is different for each sample. Because the amount of Ga on the surface is very similar it depends on the geometry of the Ga nanoparticles (this was shown in [43]). I have calculated the enhancement factor of each measured sample and the result is in the Figure 5.10. The enhancement factor of both the G band a 2D band is increasing with the Ga nanoparticle size and it shows similar value for both peaks. The D peak was not analyzed because it was nearly not measurable on the native SiO_2.

The Raman measurements were also done on graphene with Ga which was transferred on the silicon with 280 nm of SiO_2. At first I have analyzed the sample where Ga was deposited at 300 °C for 60 min. In Figure 5.11 a Raman spectroscopy map of this sample is shown. During the Ga deposition, part of the graphene sheet was covered by a molybdenum plane and therefore I have been able to measure the interface of an area with a blank graphene and an area with a graphene with deposited Ga. The map in Figure 5.11 shows the intensity of the carbon peaks. In every point of the map an information about the whole Raman spectrum related to carbon is contained. Figure 5.11 shows the Raman map of a single graphene flake with (without) Ga in upper (lower) panel, respectively. Measurements of the other graphene flakes on the sample yielded nearly identical graphs.

After the Ga deposition, the intensity of the D peak has increased significantly which indicates a number of distortions in the graphene sheet. The normalized Raman measurements are shown in the Figure 5.13. There is also a significant shift of the 2D and G peak (see Figure 5.12). The G peak has after the deposition an asymmetric shape with the maximum shifted to the lower wavenumbers for 20 cm^{-1}. The 2D peak is also shifted the lower wavenumbers for 30 cm^{-1}.

The intensities of the 2D peak and G peak were both increased by the factor of 1.8 on the sample with deposited Ga at 300 °C for 60 min. The enhancement factor is thus lower then in the case of silicon with native SiO_2. I have also prepared another sample where the gallium was deposited at 300 °C for 180 min. The amount of gallium on the surface was then three times higher and the average width of the spheres increased from 45±2 nm to 90±4 nm. The enhancement factor for this sample was 7 and 6 for G and 2D peak respectively which is shown in Figure 5.13. This is an expected result which corresponds to the results on the silicon with native SiO_2 that the enhancement factor is increasing with the size of the Ga structures on the surface. Nevertheless the enhancement factor is generally lower on the sample with 280 nm SiO_2 then on the sample with native SiO_2.

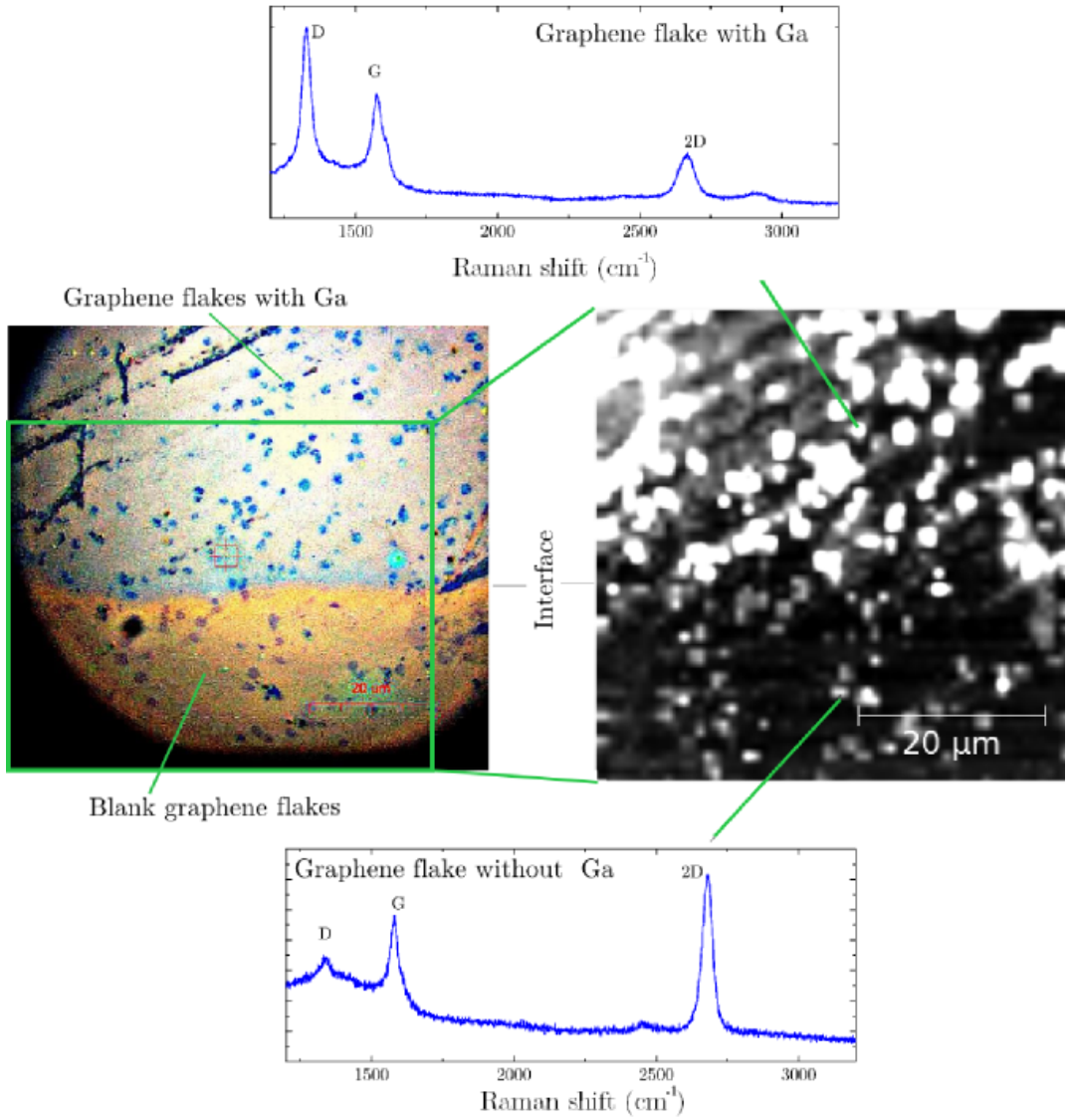

FIGURE 5.11: Left – optical microscopy image of an interface of an area with blank graphene flakes and area with flakes covered by Ga. Right – the Raman spectroscopy map of this place with a measured spectrum on each side.

5.3 Ga deposition on graphene on a copper foil

In this part I will focus on comparing the Ga deposition on the transferred CVD graphene to the Ga deposition on the graphene deposited on copper foil. As mentioned earlier the graphene sheet properties are slightly changed when the graphene is transferred with PMMA. The quality of the graphene on copper is the highest achieved in this study with no impurities present. This affects the overall adsorption properties.

I have made several experiments with graphene monocrystals prepared on the copper foil. I have deposited gallium for 60 min with a deposition rate of 0.2ML (flux current 80 nA) on these substrates. Because annealing by a direct current was not possible with these substrates I have mounted the copper foils on the top of the Si(111) with a native SiO_2 substrate. Afterwards I was able

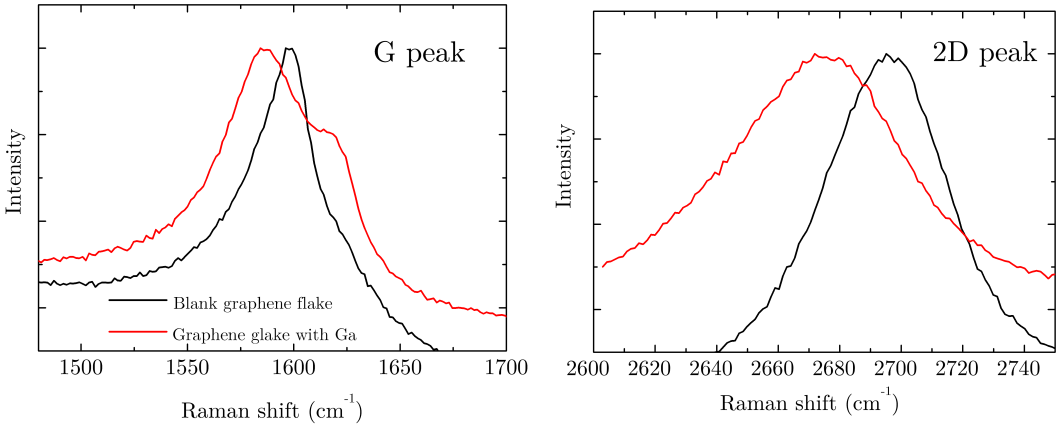

FIGURE 5.12: The shift of G and 2D Raman peak which was caused by the deposition of Ga for 60 min at 300 °C.

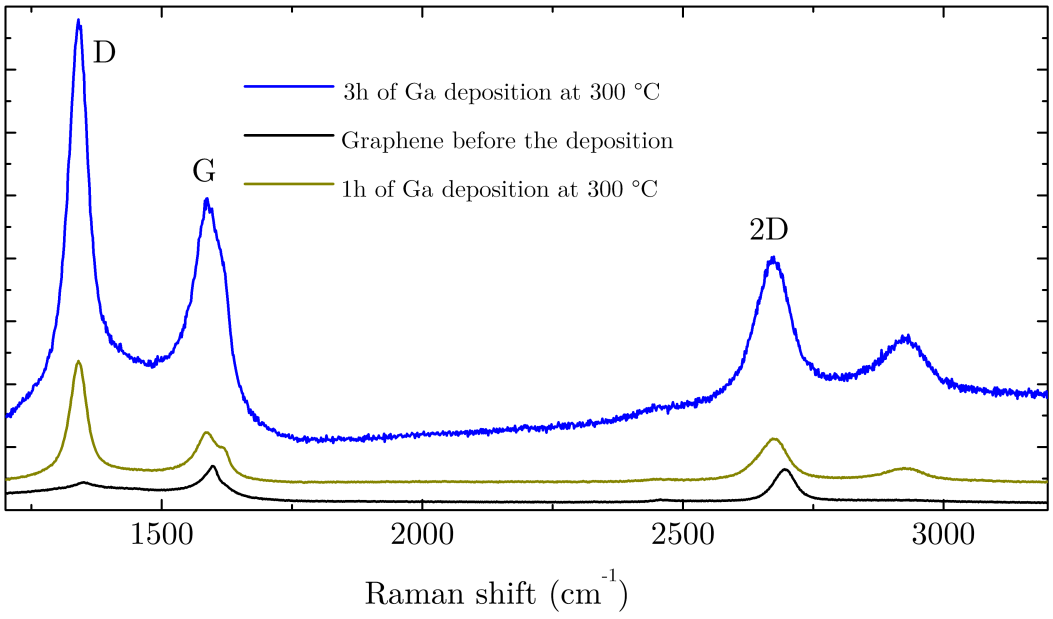

FIGURE 5.13: Raman spectra of a blank graphene (black), graphene with deposited Ga for 1 h at 300 °C (green) and graphene with deposited Ga for 3 h at 300 °C (blue). Spectra were normalized to the second overtone of silicon.

to anneal the silicon substrate by a direct current and the copper foil was then heated by the silicon substrate. At first I have annealed the substrates at 400 °C for at least 180 min. The temperature was measured by an optical pyrometer on the silicon part of the substrate. I have used only one mounting silicon substrate to ensure that by passing the same current through the silicon substrate it has nearly the same temperature for all the experiments. After the annealing I have deposited Ga at RT, 200 °, C 300 °C, and 400 °C.

I have done XPS and SEM measurements on all of the samples. XPS has confirmed the presence of Ga on all the samples. The intensity of Ga $2p_{3/2}$ was decreasing with the increasing temperature used for the sample growth. This is

expected even though it is possible that part of the signal comes from the gallium on the SiO_2.

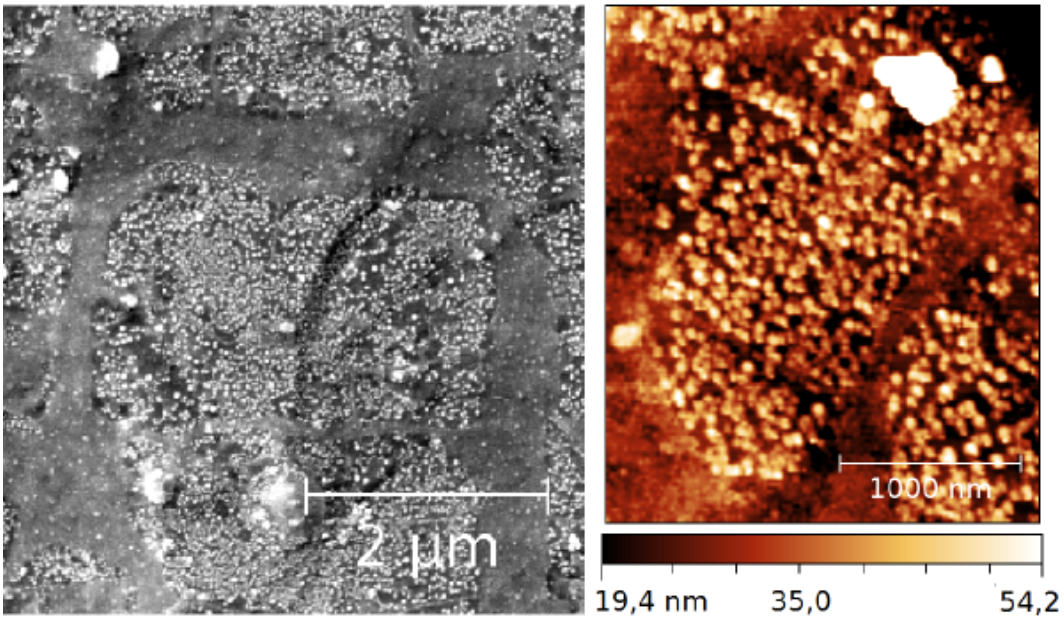

FIGURE 5.14: SEM and AFM measurements of graphene flakes on copper foil with deposited Ga at RT for 60 min.

The SEM data has surprisingly shown that the Ga spheres are present only on the RT sample (see Figure 5.14). At the higher temperatures no Ga features were observed even though the XPS measurements has shown that Ga is present on the surface. The most probable explanation is that diffusion length of gallium on pristine graphene at higher temperature (above 200 °C) is high. The impinging Ga atom diffuses on the surface until it hits the border of the monocrystal. Beyond the border there is a clean Cu foil into which the Ga atoms diffuse. This leads to a blank graphene monocrystals at the higher temperatures. The growth of Ga planes was not observed at any temperature for graphene prepared on copper foils. The Ga spheres are present only at the RT where the diffusion length is not high.

In comparison with Ga deposited on the transferred graphene sheet there is a difference in the substrate quality which enables such a high diffusion length on the graphene on the copper foil. The absence of surface defects and PMMA residues enhances the diffusion characteristics of the Ga on this surface.

5.4 Deposition of Ga on exfoliated multilayer graphene

I have also studied an adsorption of Ga on an exfoliated multilayer graphene to compare it with the adsorption of Ga on CVD-deposited graphene. The sample was prepared by a mechanical exfoliation of the highly ordered pyrolytic graphite (HOPG). The Scotch tape was used to peel off the graphite flakes which were transferred on the silicon Si(100) with 280 nm of SiO_2. The sample

was investigated by an optical microscope and a number of graphite and multilayer graphene flakes were observed on the surface. The sample was inserted in the UHV and annealed at 450 °C for 120 min. Afterwards Ga was deposited for 60 min with the flux current 80 nA at 300 °C. The sample was afterwards analyzed by SEM.

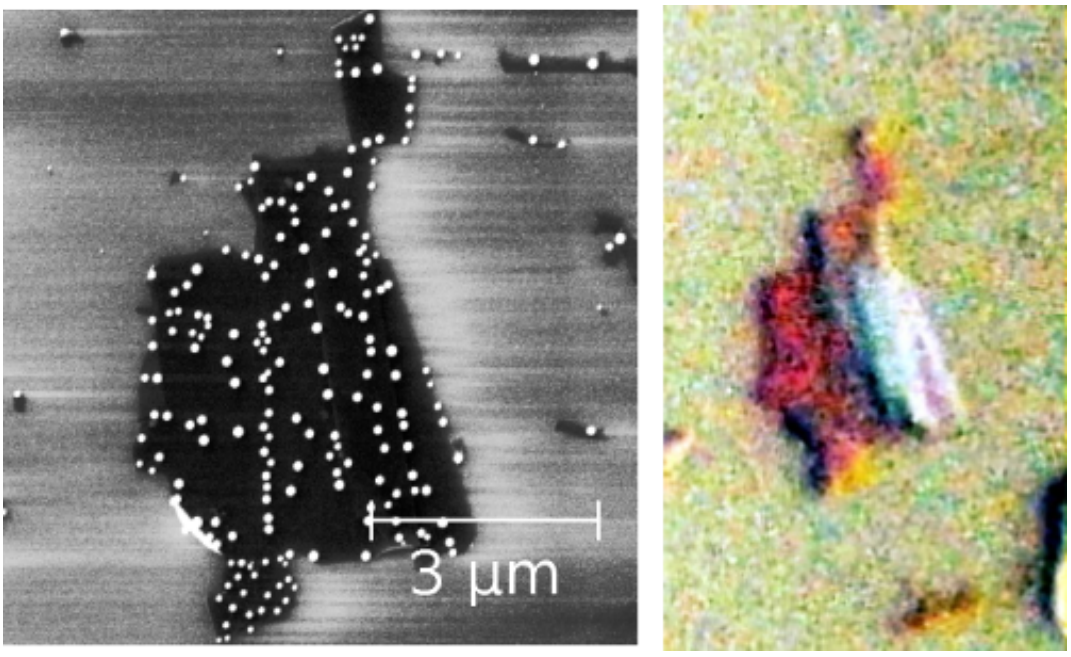

FIGURE 5.15: Left – SEM image of a multilayer graphene/graphite flake with Ga deposited at 300 °C for 60 min. Right – Image of the same flake on the optical microscope prior to the deposition.

Figure 5.15 shows the SEM measurement of the multilalyer graphene/-graphite flake. This flake was prior to the deposition inspected by the optical microscope. The flake was identified as a graphite with areas of the multilayer graphene (the pale pink areas are the multilayer graphene). As mentioned earlier the surface quality of the exfoliated graphene is excellent. After the deposition of gallium the Ga spheres were observed on the surface.

The spheres nucleated along the ridges of the graphene and graphite areas. The growth of the Ga planes was not observed in this sample. The single-layer graphene was unfortunately not obtained but it is expected for the multilayer graphene and graphite to have similar surface properties for the adsorption of Ga. This indicates that the growth of the spheres is really connected to the pristine graphene and to its surface quality. The growth of the planes is thus connected to the residues of the PMMA on the CVD-grown graphene.

The average width of the spheres on the multilayer graphene flakes on this this sample was 110±11 nm. This is much higher then in the case of transferred CVD graphene where Ga was deposited at the same conditions (average width was 45±3 nm). However the average width of the Ga spheres on the SiO_2 areas of both samples was 21±2 nm. This is very similar result to the average width of the Ga spheres on the 300 °C transferred CVD-graphene sample. This indicates that the temperature was nearly the same. The diffusion length of the Ga on

the exfoliated graphene is therefore higher than the diffusion length of Ga on the transferred CVD-graphene samples. The higher width of the Ga spheres can be therefore related to the absence of the Ga planes. If the Ga planes are not present, all the Ga material forms the Ga spheres. The surface of exfoliated graphene has no defects and no impurities and for this reason the diffusion length is most likely higher than in the case where the Ga planes occur.

6 Deposition of GaN on graphene sheets

For the deposition of GaN, an electron-impact type ion source is used (see Figure 6.1). In this type of ion source a heated tungsten wire is used to emit electrons which are afterwards accelerated to the anode [59]. These electrons can ionize the molecule of nitrogen (which is brought into the ion source by a leak valve) and create thus N_2^+ ions. These positive particles are afterwards accelerated towards the sample at a low energy (50 eV) providing a beam of N_2^+ ions (current density c.a. $1\,\mu A/cm^2$).

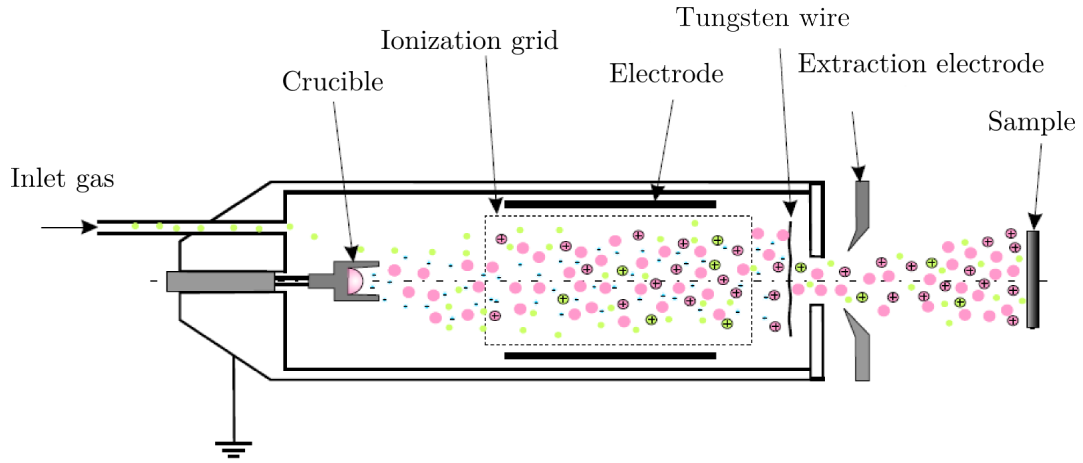

FIGURE 6.1: The schematics of an electron-impact nitrogen ion source. Image taken from [59].

I will present the measurements of one of the GaN samples I have prepared. The GaN growth is realized by the postnitridation method. As a substrate, graphene monocrystals on Si(111) with native SiO_2 were used. At first the substrate was annealed at 400 °C overnight and afterwards gallium was deposited on the sample by an evaporator with 80 nA flux current for 60 min at 300 °C. These parameters were chosen because the substrate prepared with these parameters has shown sufficiently large gallium nanostructures which are suitable for the postnitridation. After the deposition of gallium the postnitridation started. A broad beam of N_2^+ ions with the energy 50 eV was irradiating the sample. The low energy of the ions is sufficiently large for the dissociation of the N_2 molecule (dissociation energy = 9.76 eV) on the surface. The created nitrogen ion can afterwards make a bond with gallium on the surface. GaN molecule is formed on the gallium

droplet surface and it can diffuse over the surface of the Ga droplet. It can eventually nucleate at the base of the Ga sphere. This process continues until a GaN nanocrystal is formed in the place of a former gallium droplet, it was used e.g. in [60].

I have performed XPS measurements of this sample. In Figure 6.2 there are three XPS measurements of a Ga $2p_{3/2}$ peak. The black curve was measured right after the deposition of gallium and it shows only one narrow peak at 1117 eV and it corresponds only for the metallic gallium. The red curve shows the same sample after 120 minutes of nitridation by a nitrogen ion beam. The current density of this ion beam was $0{,}7\,\mu A/cm^2$ as measured by Faraday cup. It shows a broad peak which is consisting of two different peaks. The first is a metallic gallium peak at 1117 eV and the second is at 1118.7 eV. The 1118.7 eV peak comes from GaN. The ratio of the areas of these two peaks shows a relative occurrence of these two features. In Figure 6.3 the peak is fitted with a known peak parameters in XPSPeak software and it shows that there is 27% of metallic Ga and 73% of GaN on the surface.

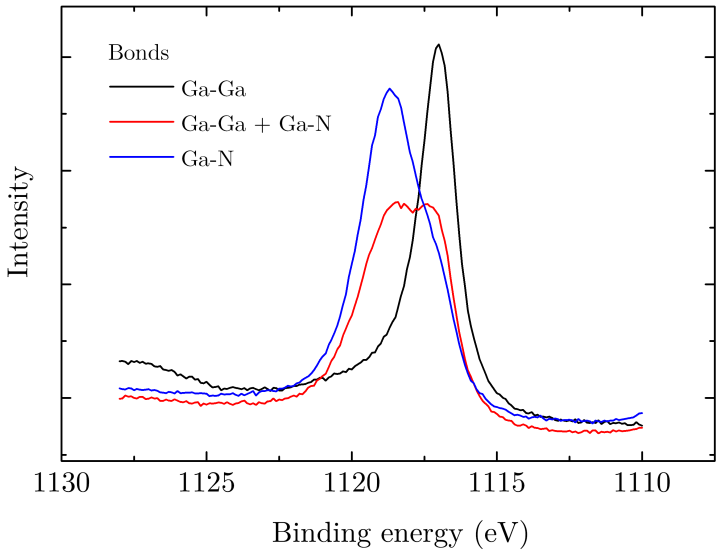

FIGURE 6.2: The evolution of the Ga $2p_{3/2}$ peak during the nitridation of Ga spheres. The black curve shows the peak after the Ga deposition. The red curve shows the peak in the middle of nitridation and the blue curve shows the peak after the nitridation was finished.

The blue curve in Figure 6.2 shows the last step of the nitridation after another two hours of nitrogen ion beam irradiation at the same conditions. The peak is also fitted in Figure 6.3 and it is shown that 88% of the Ga on the surface is GaN and only 12% of Ga on a surface stays in a metallic form with a Ga-Ga bond.

The 12% of the metalic gallium was the least amount of Ga-Ga on the surface I was able to achieve. If the nitridation proceeded for a longer time, then the decrease of the Ga-Ga percenatage would be only minor. This is related to the mechanism of the nitridation. In a certain point the growing GaN crystal can

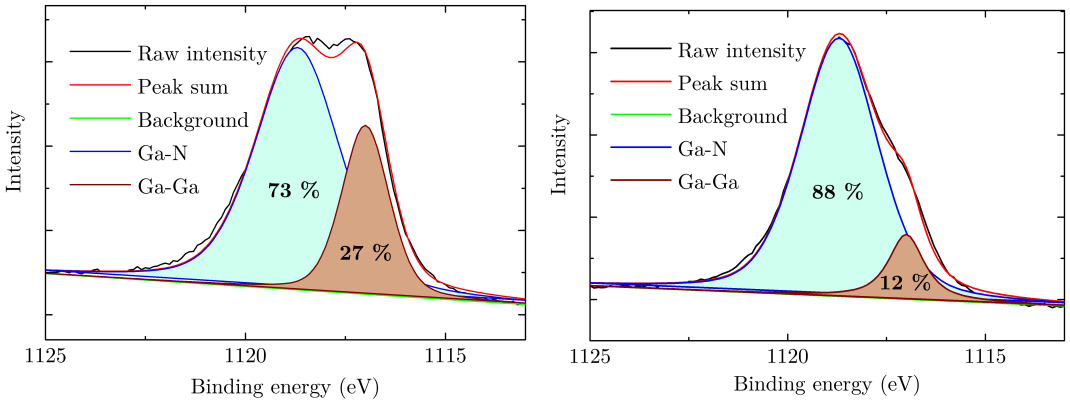

FIGURE 6.3: Left – Ga $2p_{3/2}$ peak after two hours of nitridation. Right – Ga $2p_{3/2}$ peak after the nitridation was finished.

cover the Ga-residues and the impinging nitrogen ion cannot bind to a Ga atom on the structure anymore. This can be overcome by the deposition of smaller Ga spheres.

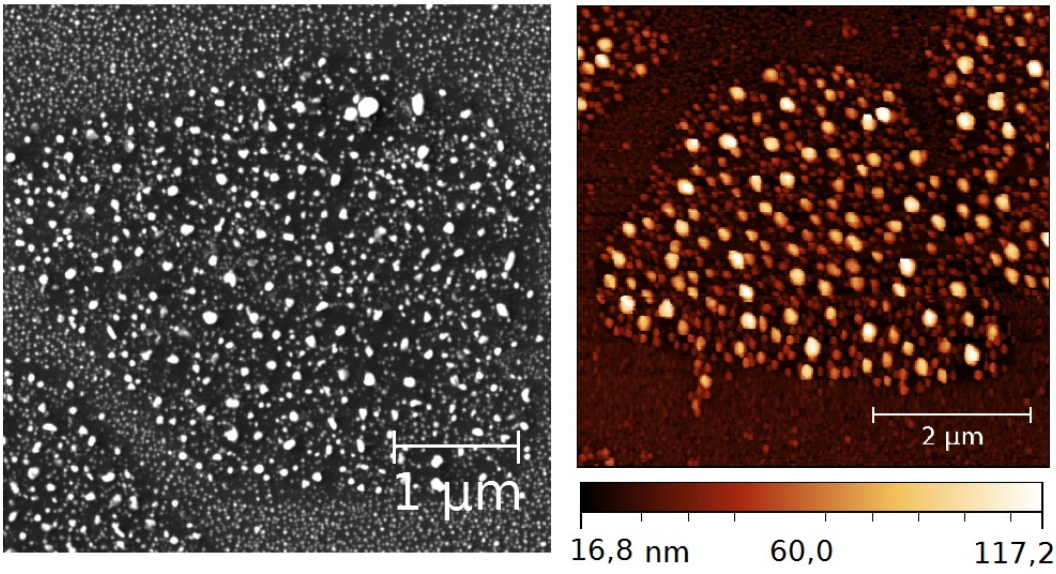

FIGURE 6.4: SEM(left) and AFM(right) measurements of a graphene flake with deposited GaN.

AFM and SEM measurements of the graphene with deposited GaN are in Figure 6.4. The geometry of the structures on this graphene surface corresponds to the geometry of the Ga structures which were deposited at 300 °C in previous chapter. Theses Ga structures are transformed to the GaN structures which are of a similar size like the original Ga structures. Similarly to Ga structures, two kinds of GaN structures are found – spheres and planes. Furthermore, the GaN structures on the SiO_2 are also very similar to the structures observed in the previous chapter. It can be concluded that the morphology of GaN structures is rather similar to the morphology of Ga structures used for the nitridation.

Nevertheless, the electronic structure and the chemical composition of these Ga structures has changed substantially from a metal to a semiconductor. This has an impact for the Raman measurements of the carbon peaks. Figure 6.5 shows the Raman spectrum of the carbon peaks of graphene with the GaN together with a spectrum of a blank graphene sheet. It can be seen that there is no substantial enhancement of the intensity of the Raman peaks. This is also an expected result. The transformed Ga sphere cannot serve as a source of the SERS effect anymore. Because the graphene was transferred onto the silicon with native SiO_2, the overall intensity of the carbon peaks is low.

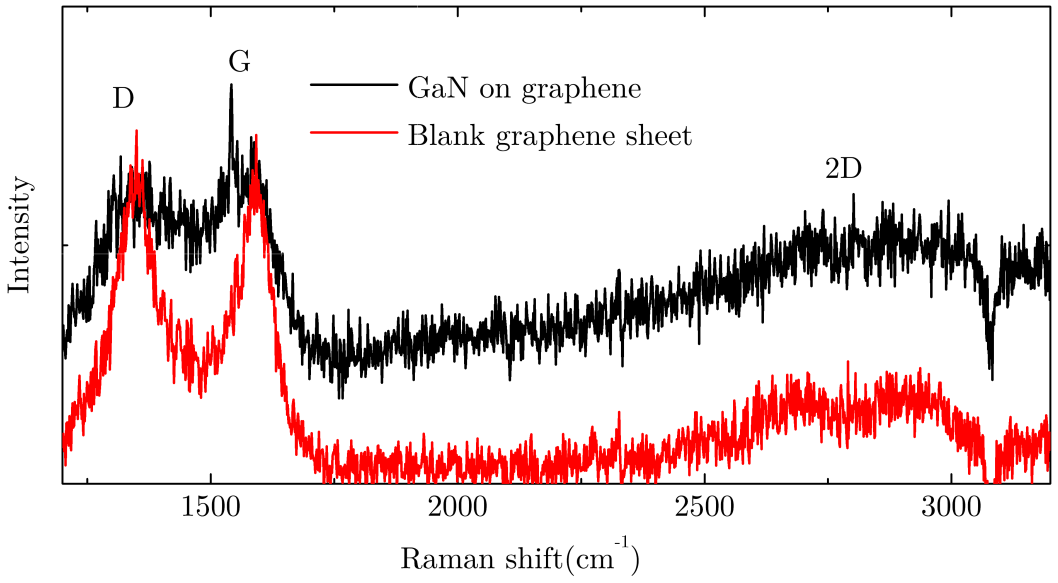

FIGURE 6.5: Raman spectrum of a blank graphene sheet on the native SiO_2 and the Raman spectrum of the same sample after the deposition of GaN.

I have measured the photoluminescence (PL) spectra on this sample. A good photoluminescence response of GaN is highly desirable as most of GaN applications are from the field of optoelectronics. Unfortunately on this sample the photoluminescence was not measurable . The measured spectrum is in the Figure 6.6. GaN has a bandgap of 3.39 eV at the room temperature and therefore the PL maximum should be around 365 nm. For this reason a 325 nm UV laser was used for an excitation. Figure 6.6 shows the PL spectrum of a clean silicon with native SiO_2 and the PL of the GaN sample which was deposited on graphene on the native SiO_2. There are a few distinct peaks in these two spectra but these are related to the silicon substrate and they are identical. For this reason it can be stated that the GaN microcrystals have a number of dislocations which damage the bulk structure of the crystals and provide a strong non-radiative recombination channel which quenches the photoluminescence. Other possibility is that the PL intensity is too low to be measured or that there is a lot of impurities in the GaN bulk. The PL spectra can be possibly enhanced by the deposition of large GaN structures.

I was especially interested in the XPS measurements of the graphene because I wanted to measure the effects of the deposited Ga and the deposited GaN

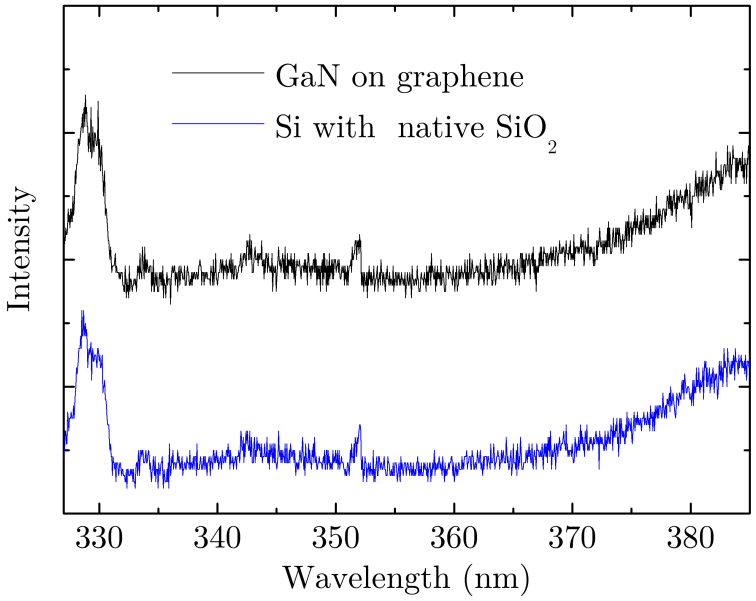

FIGURE 6.6: Photoluminescence spectra of GaN on graphene and silicon with native SiO_2. No GaN-related photoluminescence was observed. The offset of the spectra is artificial.

on the graphene valence band. I was inspired by [43] where similar measurements were shown with a high coverage of Ga.

Figure 6.7 shows the results of this effort. The red curve shows the XPS measurement of an annealed pristine graphene. The blue curve shows the XPS measurement in a valence band after the deposition of Ga at 300 °C. The green curve shows the same measurement after two hours of nitridation of this sample and the black curve shows the spectrum of the sample which was obtained after the nitridation was finished. The annealed graphene shows several peaks which correspond to [43]. It shows the C 2p π states at 4 eV and the crossing of C 2p π and C 2p σ states at 6 eV. After the deposition of Ga an intensive Ga 3d peak occurs at 18 eV and there is another peak at 8 eV which comes also from Ga. Also the metallic states of Ga are present around 0 eV. After two hours of nitridation the peaks are shifted to the higher binding energies and when the nitridation is finished the Ga peaks stop their shift towards the higher binding energies. Ref. [43] states that if the Ga was bonded to C forming C-Ga states the C 2p π band would be decreased with increasing Ga coverage. The signature of bonding was not found in our spectra and we conclude that the graphene structure is not pronouncedly affected by the deposited Ga. We note that the Ga-related increase at 8 eV and the Ga 3d peak were not discussed in [43].

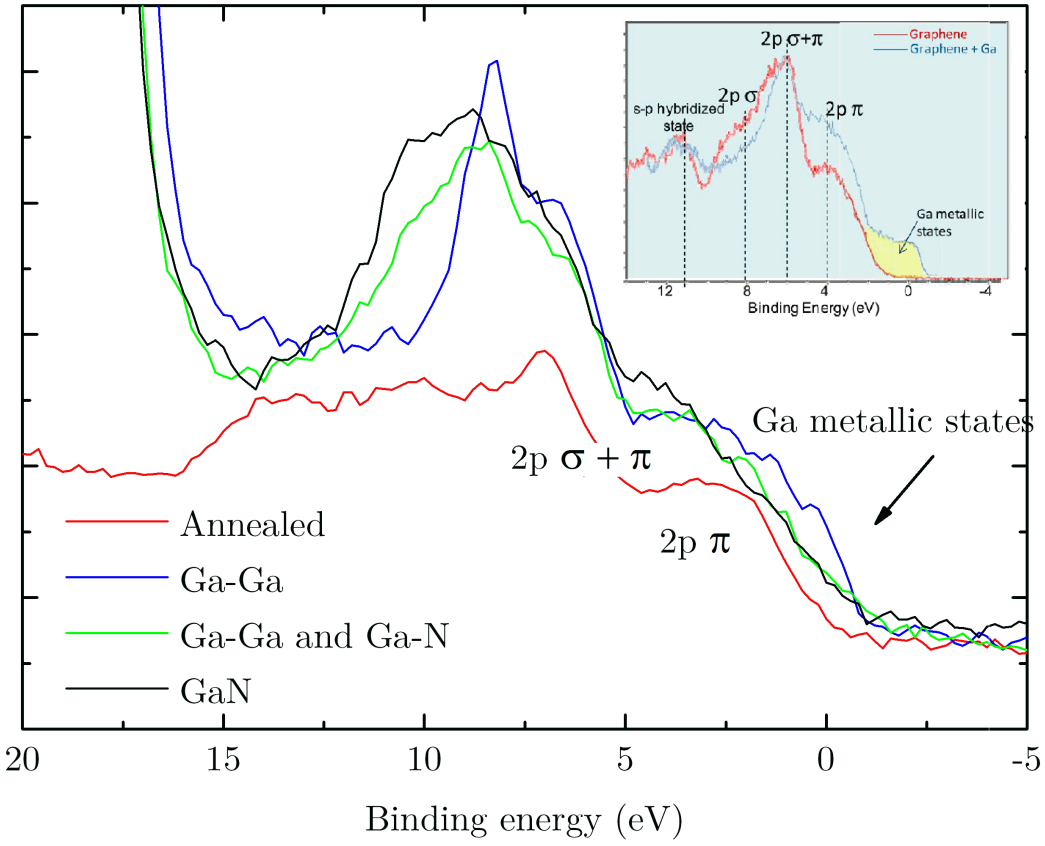

FIGURE 6.7: The XPS spectrum of a graphene's valence band. It shows the spectrum of an annealed graphene, graphene with deposited Ga, graphene with deposited Ga after two hours of nitridation and graphene with GaN. The image in upper right corner is taken from [43]

Summary

I have studied the properties of the Ga and GaN nanostructures on the transferred CVD graphene substrate. The main goal of my thesis was to investigate the properties of evaporated Ga on this substrate. The GaN was fabricated by the one-step nitridation of the Ga structures and this suitable method enabled me to study the properties of both Ga and GaN structures on the sample.

In the theoretical part of my work I have introduced the problematics of the fabrication of the high quality GaN and graphene. I have also focused on the latest scientific achievements in the field of graphene and its relation to the Ga and GaN. The study of the metal nanoparticles on graphene is an expanding area of interest. The importance of graphene for the fabrication of GaN layers and for the application of the GaN-based devices was discussed as well.

In the experimental part of my work I have focused mostly on the adsorption of Ga on the transferred CVD-graphene. For this reason in the first step I had to investigate the properties of the CVD graphene substrate prior to the transfer onto an SiO_2 and after this transfer. This was done by AFM, SEM, XPS and the Raman spectroscopy measurements. The measurements showed that the character of the graphene prior to the transfer is pristine. The process of the transferring introduces impurities from the PMMA on the graphene sheets. Furthermore the graphene sheet is strained during the transfer which results in cracking of the large graphene sheet. I have also discussed the differences between the native SiO_2/Si and 300 nm SiO_2/Si substrates manifested in Raman spectroscopy measurements.

With this knowledge I have performed a series of depositions of Ga on these substrates at various temperatures. Gallium forms two types of structures on the transferred graphene sheets: spheres and planes. I have presented a dependence of the size of the Ga spheres on the deposition temperature and I have compared it with the same dependence on the SiO_2. It showed that the diffusion length of the Ga on graphene is significantly higher than the diffusion length on the SiO_2. I have also studied the structure of the Ga planes by an energy dispersive X-ray spectroscopy and it was confirmed that the planes are composed of Ga. However the exact principle of their formation is not known but it is presumed that the growth of the Ga planes is strongly connected to the PMMA residues on graphene.

The Raman spectroscopy of the graphene samples covered with Ga structures deposited on graphene substrate showed that the presence of Ga particles strongly influences the Raman spectrum. The magnitude of the D peak is strongly increased after the deposition of Ga and also the position of the G and 2D peak is shifted. Furthermore the samples exhibit a strong SERS effect. The overall

intensity of the Raman spectrum was increased by the presence of the Ga NPs. The magnitude of the increase was dependent on the size of the deposited particles and this dependence was also presented. The differences of the native SiO_2/Si and 300 nm SiO_2/Si substrates for these Raman spectrum measurements were illustrated here as well.

To acquire more information about the Ga and the substrates I have also compared the depositions of Ga on the transferred CVD graphene with the depositions of Ga on the exfoliated multilayer graphene and on the graphene on the copper foil. The results showed that the adsorption on these substrates exhibits major differences. The depositions of Ga on the graphene on the copper foil, which has a great quality, showed that on the pristine graphene the diffusion length of the Ga is high and the Ga particles most likely diffuse into the copper at temperatures higher then 200 °C. The experiment with the exfoliated graphene showed that no Ga planes are formed on the surface which confirms the idea that the growth of the Ga planes is related to the PMMA residues. Also the diffusion length of Ga on this substrate was higher than on the transferred CVD graphene.

These experiments have shown that the quality of the transferred CVD graphene is still not sufficient for a good quality GaN depositions and that the process of the graphene transfer needs to be improved. However it was still possible to reveal the basic properties of the Ga on graphene.

I have also inspected the formation of GaN on graphene. After the evaporation of the Ga on the transferred CVD graphene the Ga structures were nitridated by the nitrogen ion source. I have discussed the XPS measurements at several stages of this process and I have presented the XPS measurements of graphene's valence band during the formation of GaN. I have also showed the AFM, SEM, Raman spectroscopy and the photoluminescence spectra of the GaN sample. The quality of the deposited GaN was discussed based on these measurements. The GaN deposition method parameters need to be tuned to achieve high-quality GaN crystals.

Bibliography

[1] U.S. Geological Survey: Gallium statistics and information - 2013. *USGS website*, URL `http://minerals.usgs.gov/minerals/pubs/commodity/gallium/mcs-2013-galli.pdf`, 13 April 2014.

[2] Munoz-Tabares J.A., Anglada M. , Reyes-Gasga J.: Deposition of metallic gallium on re-crystallized ceramic material during focused ion beam milling. *Materials Characterization*, Volume 86, Pages 92 – 96, 2013.

[3] Jo. M., Mano T., Sakuma Y., Sakoda K.. Size-dependent contact angle of Ga droplets on GaAs. *Journal of Crystal Growth*, Volume 378, pp 5 – 7, 2013.

[4] Kolíbal M., Čechal T., Brandejsová E., Čechal J., Šikola T.: Self-limiting cyclic growth of gallium droplets on Si(111). *Nanotechnology*, Volume 19, Number 47, 2008.

[5] Čechal J., Matlocha T., Polčák J., Kolíbal M., Tomanec O., Kalousek R., Dub P., Šikola T.: Characterization of oxidized gallium droplets on silicon surface: An ellipsoidal droplet shape model for angle resolved X- ray photoelectron spectroscopy analysis. *Thin Solid Films*, Volume 517, Number 6, pp. 1928 – 1934, 2009.

[6] Du K., Glogowski E., Tuominen M. T., Emrick T., Russel T. P., Dinsmore A. D.: Self-assembly of gold nanoparticles on gallium droplets: Controlling charge transport through microscopic devices. *Langmuir*, Volume 29, pp. 13640 – 13646, 2013.

[7] Elborg M., Noda T., Mano T., Jo. M., Sakuma Y., Sakoda K.: Self-assembly of Ga droplets attached to GaAs quantum dots. *Journal of Crystal Growth*, Volume 378, pp. 53 – 56, 2013.

[8] Feng Z. C.: III-Nitride Semiconductor Materials. *Imperial College Press*, 2006.

[9] Coleman J.J., Bryce A.C., Jagadish C.: Advances in Semiconductor lasers. *Academic Press*, 2012.

[10] Kirilyuk, V.: Optical characterization of gallium nitride. PhD thesis, University of Nijmegen. *Imperial College Press*, 2002.

[11] Nakamura S., Pearton S., Fasol G.: The blue laser diode: The complete story. *Springer*, 2000.

[12] Lagerstedt O., Monemar A.: Variation of lattice parameters in GaN with stoichiometry and doping. *Journal of Applied Physics*, Volume 45, 1974.

[13] Bougrov V., Levinshtein M., Rumyantsev S., Zubrilov A.: Properties of Advanced Semiconductor Materials: GaN, AIN, InN, BN, SiC, SiGe. *Wiley*, pp. 1 – 28, 2001.

[14] Grzegory I.: High pressure growth of bulk GaN from solutions in gallium. *Journal of Physics: Condensed Matter*, Volume 13, Number 32, 2001.

[15] Fernandéz-Garrido S., Koblmüller G., Calleja E., Speck J. S.: In situ GaN decomposition analysis by quadrupole mass spectrometry and reflection high energy electron diffraction. *Journal of applied physics*, Volume 13, 033541, 2008.

[16] Kukushkin S.A., Osipov A.V., Bessolov V.N., Medvedev B.K., Nevolin V.K., Tcarik K.A.: Substrates for epitaxy of gallium nitride: New materials and techniques. *Reviews on Advanced Materials Science*, Volume 17, pp. 1 – 32, 2008.

[17] Liu L., Edgar J.H.: Substrates for gallium nitride epitaxy. *Materials Science and Engineering*, R 37,pp. 61 – 127, 2002.

[18] Van Nostrand J.E., Solomon J., Saxler A. Xie Q., Reynolds D.C., Look D.C.: Dissociation of Al_2O_3(0001) substrates and the roles of silicon and oxygen in n-type GaN thin solid films grown by gas-source molecular beam epitaxy. *Journal of applied physics*, Volume 87, 8766, 2000.

[19] Zhu D., Humphreys C.J.: Low-cost high-efficiency GaN LED on large-area Si substrate . *CS MANTECH Conference 2013*, manuscript, Volume 87, 8766, 2000. Available from: `http://www.csmantech.org/Digests/2013/papers/078.pdf`.

[20] Gupta V.K., Averett K.L., Koch M.W., McIntyre B.L., Wicks G.W.: Selective area growth of GaN using gas source molecular beam epitaxy. *Journal of Electronic Materials*, Volume 29, Number 3, 2000.

[21] Fortuna S.A., Li X.: Metal-catalyzed semiconductor nanowires: A review on the control of growth directions. *Semiconductor Science Technologies*, Volume 25, 054005, 2010.

[22] Wagner R.S., Ellis W.C.: Vapor-liquid-solid mechanism of single ctystal growth. *Applied Physics Letters*, Volume 4, pp. 89 – 90, 1964.

[23] Purushothaman V., Ramakrishnan V., Jeganathan K.: Interplay of VLS and VS growth mechanism for GaN nanowires by a self-catalytic approach. *RSC Advances*, Volume 2, pp. 4802 – 4806, 2012.

[24] Ma Z., McDowell D., Panaitescu E., Davydov A.V., Upmanyu M., Menon L.: Vapor-liquid-solid growth of serrated GaN nanowires: Shape selection driven by kinetic frustration. *Journal of Materials Chemistry C*, Volume 1, 7294, 2013.

[25] Fernández-Garrido S., Grandal J., Calleja E., Sánchez-García M.A, Lopez-Romero D.: A growth diagram for plasma-assisted molecular beam epitaxy of GaN nanocolumns on Si(111). *Journal of Applied Physics*, Volume 106, pp. 126102, 2009.

[26] Novoselov K.S., Geim A.K., Morozov S.V., Jiang D., Zhang Y., Dubonos S.V., Grigorieva I.V., Firsov A.A.: Electric field effect in atomically thin carbon films. *Science*, Volume 306, Number 5696, pp. 666 – 669, 2004.

[27] Cooper D.R., D'Anjou B., Ghattamaneni N., Harack B., Hilke M., Horth A., Majlis N., Massicotte M., Vandsburger L., Whiteway E., Yu V.: Experimental review of graphene. *International Scholarly Research Network*, Volume 2012, pp. 501686, 2011.

[28] Geim A.K.: Graphene: Status and Prospects. *Science*, Volume 324, Number 5934, pp. 1530 – 1534, 2009.

[29] Nair R.R., Blake P., Grigorenko A.N., Novoselov K.S., Booth T.J., Stauber T., Peres N.M.R., Geim A.K.: Fine structure constant defines visual transparency of graphene. *Science*, Volume 320, Number 1308, pp. 1530 – 1534, 2009.

[30] Hibino H., Kageshima H., Nagase M.: Graphene Growth on Silicon Carbide. *NTT technical Review*, Volume 8, Number 8, 2010.

[31] Zhang Y., Zhang L., Zhou C.: Review of chemical vapor deposition of graphene and related applications. *Accounts of chemical research*, Volume 46, Number 10, pp. 2329 – 2339, 2010.

[32] Trinsoutrot P., Vergnes H., Caussat B.: Three dimensional graphene synthesis on nickel foam by chemical vapor deposition from ethylene. *Materials Science and Engineering: B*, Volume 179, pp. 12 – 16, 2014.

[33] Han H.G., Gunes F., Bae J.J., Kim E.S., Chae S.J., Shin H., Choi J., Pribat D., Lee Y.H.: Influence of copper morphology in forming nucleation seeds for graphene growth. *Nano Letters*, Volume 11, pp. 4144 – 4148, 2011.

[34] Procházka P.: The preparation of graphene by method CVD. *Master's thesis*, Brno University of Technology, 2012.

[35] Kumar A., Lee C.H.: Synthesis and biomedical applications of graphene: Present and future trends. *Advances in graphene science*, InTech, 2013.

[36] Ferrari A.C., Basko D.M.: Raman spectroscopy as a versatile tool for studying the properties of graphene. *Nature Nanotechnology*, Volume 8, pp. 235 – 246, 2013.

[37] Wikipedia contributors: Raman spectroscopy. *Wikipedia, The Free Encyclopedia*, 25 May 2014. URL `http://en.wikipedia.org/w/index.php?title=Raman_spectroscopy&oldid=605688559`.

[38] Childres I., Jauregui L.A., Park W., Cao H., Chen Y.P.: New developments in photon and materials research: Raman spectroscopy of graphene and related materials. *Nova Science Publishers*, Chapter 19, 2013.

[39] Ferrari A.C.: Raman spectroscopy of graphene and graphite: Disorder, electron-phonon coupling, doping and nonadiabatic effects. *Solid State Communications*, Volume 143, Issues 1 – 2, pp. 47 – 57, 2007.

[40] Wang C., Ye F., Wu H., Qian Y.: Depositing Au nanoparticles onto graphene sheets for simultaneous electrochemical detection ascorbic acid dopamine and uric acid. *International Journal of Electrochemical Science*, Volume 8, pp. 2440 – 2448, 2013.

[41] Sidorov A.N., Slawinski G.W., Jayatissa A.H., Zamborini F.P., Sumanasekera G.U.: A surface-enhanced Raman spectroscopy study of thin graphene sheets functionalized with gold and silver nanostrucutres by seed-mediated growth. *Carbon*, Volume 50, pp. 699 – 705, 2012.

[42] Wu Y., Jiang W., Ren Y., Cai W., Lee W.H., Li H., Piner R.D., Pope C.W., Hao Y., Ji H., Kang J., Ruoff R.S.: Tuning the doping type and level of graphene with different gold configurations. *Small*, Volume 8, pp. 3129 – 3136, 2012.

[43] Losurdo M., Congwen Y., Suvorova A., Rubanov S., Kim T., Giangregorio M.M., Jiao W., Bergmair I., Bruno G., Brown A.S.: Demonstrating the capability of the high-performance plasmonic gallium-graphene couple. *ACS Nano*, Volume 8, pp. 3031 – 3041, 2014.

[44] Plant S.R., Cao L., Yin F., Wang Z.H., Palmer R.E.: Size-dependent propagation of Au nanoclusters through few-layer graphene. *Nanoscale*, Volume 6, pp. 1258 – 1263, 2014.

[45] Sharma S., Verma A.S.: A theoretical study of H_2S adsorption on graphene doped with B, Al and Ga. *Physica B*, Volume 427, pp. 12 – 16, 2013.

[46] Luo Z., Shang J., Lim H., Li D., Xiong Q., Shen Z., Lin J., Yu T.: Modulating the electronic structures of graphene by controllable hydrogenation. *Applied Physics Letters*, Volume 97, pp. 233111, 2010.

[47] Gupta P., Rahman A.A., Hatui N., Gokhale M.R., Deshmukh M.M., Bhattacharya A.: MOVPE growth of semipolar III-nitride semiconductors on CVD graphene. *Journal of Crystal Growth*, Volume 372, pp. 105 – 108, 2013.

[48] Ishii A., Tatani T., Asano H., Nakada K.: Computational study for growth of GaN on graphite as 3D growth on 2D material. *Physica Status Solidi C*, Volume 7, Number 2, pp. 347 – 350, 2010.

[49] Gohda Y., Tsuneyuki S.: Structural phase transition of graphene caused by GaN epitaxy. *Applied Physics Letters*, Volume 100, pp. 053111, 2012.

[50] Choi J., Huh J., Kim S., Moon D., Yoon D., Joo K., Kwak J., Chu J.H., Kim S.Y., Park K., Kim Y., Yoon E., Cheong H., Kwon S.: One-step graphene coating of heteroepitaxial GaN films. *Nanotechnology*, Volume 23, Number 43, 2012.

[51] Patsha A., Sahoo P., Madapu K.K., Dhara S., Tyagi A.K.: Growth of GaN nanostructures on graphene. *International Conference on Nanoscience Engineering and Technology*, IN 978-1-4673-0071-1, 2011.

[52] Chung K., Lee C.,Yi G.: Transferable GaN Layers Grown on ZnO-Coated Graphene Layers for Optoelectronic Devices. *Science*, Volume 30, pp. 655 – 657, 2010.

[53] Lai W., Lin C., Lai Y., Yu P., Chi G.C., Chang S.: GaN-based light-emitting diodes with graphene/indium tin oxide transparent layer. *Optics Express*, Volume 22, Issue S2, pp. A396 – A401, 2014.

[54] Chung K., Park S.I., Baek H., Chung J., Yi G.: High-quality GaN films grown on chemical vapor-deposited graphene films. *NPG Asia Materials*, Volume 4, 2012.

[55] Baek H., Lee C., Chung K., Yi G.: Epitaxial GaN Microdisks Lasers Grown on Graphene Microdots. *Nano Letters*, Volume 13, pp. 2782 – 2785, 2013.

[56] Dvořák M.: Deposition of Ga and GaN ultrathin layers on graphene substrate. *Brno University of Technology*, Master's thesis , 2013.

[57] Webb M., Palgren P., Pal P., Karis O., Grennberg H.: A simple method to produce almost perfect graphene on highly oriented pyrolytic graphite. *Carbon*, Volume 49, Number 10 pp. 3242 – 3249 , 2011.

[58] Yoon D., Moon H., Son Y., Choi J.S., Park B.H., Cha Y.H., Kim Y.D., Cheong H.: Interference effect on Raman spectrum of graphene on SiO_2. *Physical Review B*, Volume 80, 125422 , 2009.

[59] Mach J.: Development and Application of an UHV Equipment for Deposition of Thin Films, *Brno University of Technology*, PhD thesis, 2009.

[60] Novák T.: Selective gallium nitride thin-film growth on substrates covered by pyrolyzed resist mask, *Brno University of Technology*, Master's thesis, 2013.